Bonriki Inundation Vulnerability Assessment

Atoll Island Hydrogeology and Vulnerability to Seawater Intrusion - A Literature Review

Adrian D Werner, Sandra Galvis Rodriguez,
Vincent E A Post, Danica Jakovovic

Australian Government

SPC Secretariat of the Pacific Community

Australian Aid

Bonriki Inundation Vulnerability Assessment (BIVA)

Atoll Island Hydrogeology and Vulnerability to Seawater Intrusion – A Literature Review

Adrian D. Werner

Sandra Galvis Rodriguez

Vincent E.A. Post

Danica Jakovovic

SPC
Secretariat
of the Pacific
Community

Original text: English

Secretariat of the Pacific Community Cataloguing-in-publication data

SPC Technical Report SPC00008

January 2015

Werner, Adrian D.

Atoll Island Hydrogeology and Vulnerability to Seawater Intrusion: a literature review / Adrian D. Werner, Sandra Galvis Rodriguez, Vincent E. A. Post and Danica Jakovovic

(Bonriki Inundation Vulnerability Assessment (BIVA) / Secretariat of the Pacific Community)

1. Sea level — Climatic factors — Kiribati.
2. Floods — Kiribati.
3. Climatic changes — Social aspects — Kiribati.
4. Climatic changes — Management — Kiribati.
5. Climatic changes — Environmental aspects — Kiribati.
6. Climate change mitigation — Kiribati.

I. Werner, Adrian D. II. Galvis Rodriguez, Sandra III. Post, Vincent E. A. IV. Jakovovic, Danica V. Title. VI. Secretariat of the Pacific Community. VII. Series

577.220 99593 AACR2

ISBN: 978-982-00-0928-8

Table of Contents

List of Tables

List of Figures

Acknowledgement

The BIVA project is part of the Australian Government's Pacific-Australia Climate Change Science and Adaptation Planning Program (PACCSAP), within the International Climate Change Adaptation Initiative. The project was developed by the Secretariat of the Pacific Community's (SPC) Geoscience Division (GSD) in partnership with the Australian Government and the Government of Kiribati (GoK).

Key GoK stakeholders that contributed to the implementation of the project were:

- Ministry of Public Works and Utilities (MPWU), in particular the Water Engineering Unit with the MPWU
- The Public Utilities Board (PUB), in particular the Water and Sanitation Division and the Customer Relations Division within the PUB
- The Office of the President, in particular the Disaster Management Office
- The Ministry of Environment, Lands and Agricultural Development (MELAD) Lands Division
- The Ministry of Fisheries and Marine Resources Development (MFMRD) Minerals Division
- Members of the Kiribati National Expert Group on climate change and disaster risk management (KNEG)

The Bonriki Village community members also played a key role in the implementation of the project. Community members participated in the school water science and mapping program, assisted with construction of new piezometers and data collection for the groundwater component, and shared their knowledge and experiences with regards to historical inundation events and coastal processes.

Key technical advisors involved with implementation of the project included:

- Flinders University, Adelaide, Australia
- University of Western Australia, Perth, Australia
- The University of Auckland, Auckland, New Zealand
- United Nations Educational, Scientific and Cultural Organization, Institute for Water Education (UNESCO-IHE), Delft, the Netherlands
- Technical advisors Tony Falkland and Ian White

Glossary

Boundary condition

Water-level or solute-concentration controls on a groundwater system around the boundary of the study area that correspond to hydrogeologic features, such as a body of surface water, an impermeable surface, or ocean.

Convection cell

A distinct volume of circulating fluid, in a fluid medium under gravity, that circulates under the effects of variations in water density. In the case of coastal aquifers, these density variations are the result of differences in salinity.

Density-dependent flow and transport processes

Where the salinity of ground water is significant, the groundwater flow and solute movement are influenced by density variations. A salinity–density relationship is used to couple the groundwater flow and solute transport equations.

Dispersion

The spreading and mixing of solutes caused by the combined effects of molecular diffusion and mechanical dispersion.

Dispersivity

An empirical parameter that defines the spread of solutes. Longitudinal dispersivity defines the spread of solutes in the direction of groundwater flow, and transverse dispersivity defines the spread of solutes perpendicular to the groundwater flow direction.

Dupuit assumption

Also known as the Dupuit-Forchheimer assumption, it is a simplifying assumption for the solution of flow in unconfined aquifers (i.e. a watertable aquifer). It is based on the assumption that the slope of the phreatic surface (i.e. the water table) is negligibly small so that the equipotential lines are vertical (i.e. hydrostatic pressure conditions), and flow is essentially horizontal if the lower boundary of the flow domain is horizontal.

Facies

A distinctive rock unit that forms under certain conditions of sedimentation, reflecting a particular process or environment.

Flux-controlled inland boundary conditions

The assumption that the rate of groundwater flow in a coastal aquifer at some inland location is known, and can be specified to find the mathematical solution to a coastal aquifer model.

Forcing function

A mathematical description of groundwater conditions, usually varying in time, along the boundary of a groundwater model.

Ghyben-Herzberg (GH) approximation

A simplified relationship defining the location of the freshwater–seawater interface in a coastal aquifer, assuming steady-state conditions, no solute mixing (i.e. a sharp interface), and hydrostatic conditions (i.e. the Dupuit assumption) that depends on the density contrast between sea water and fresh water. The GH approximation suggests that, in a coastal aquifer, the depth of fresh water below mean sea level is 40 times the height of fresh water above mean sea level, for water densities of 1,000 kg/m^3 (fresh water) and 1,025 kg/m^3 (sea water).

Head-controlled inland boundary conditions

The assumption that the hydraulic head in a coastal aquifer at some inland location is known and can be specified to find the mathematical solution to a coastal aquifer model.

Heterogeneous aquifer

An aquifer is said to be heterogeneous if its properties have significant spatial variability.

Holocene

A geological epoch that began at the end of the Pleistocene (11,700 years before present) and continues to the present.

Holocene-Pleistocene unconformity (HPU)

A buried erosional surface between sedimentary rocks from the Holocene and Pleistocene periods that presents as a discontinuity, indicating interruption of sedimentation, accompanied by erosion of rocks below the interface.

Homogeneous aquifer

The simplifying assumption that the properties of an aquifer have no spatial variability.

Hydraulic conductivity (*K*)

The aquifer property defining the rate of groundwater flow through a given cross-sectional area that arises from a given hydraulic gradient

Hydraulic gradient

The hydraulic head slope, defined as the difference in hydraulic head divided by the distance over which the head difference occurs. In unconfined aquifers, and adopting the Dupuit assumption, this is given by the slope of the watertable surface.

hydrodynamic dispersion

See 'dispersion'.

Inundation

Flooding or submergence.

Karstification

The dissolution of soluble rocks such as limestone and dolomite, forming fissures, sinkholes and caverns that provide preferential pathways for groundwater flow.

K_B/K_U ratio

The ratio between the hydraulic conductivity of the lower Pleistocene limestone (K_B) and the upper Holocene sediments (K_U). K_B/K_U is typically on the order of 100.

Mathematical groundwater model

A mathematical model describes the physical processes of a groundwater system using one or more governing equations, aquifer hydraulic properties, stresses on the aquifer (e.g. pumping, recharge), and knowledge of boundary conditions. Mathematical models can be subdivided into analytical and numerical models.

Mathematical groundwater model (analytical)

An analytical model solves highly simplified representations of aquifers (e.g. properties of the aquifer are considered to be constant in space and time, aquifer geometry is uniform) to enable a rapid solution to a given problem.

Mathematical groundwater model (numerical)

A numerical model divides space and/or time into discrete pieces, enabling more complex and potentially more realistic (relative to analytical models) representations of a groundwater system to be developed. Two dimensional cross-sectional numerical models consider only a vertical slice of the study area. Three dimensional numerical models consider areal and vertical extents of the study area.

Mechanical dispersion

The process whereby solutes are mechanically mixed during groundwater flow caused by velocity variations at the microscopic level.

Molecular diffusion

The process whereby solutes are transported at the microscopic level by the random thermal movement of molecules, resulting in solute spreading due to variations in the solute concentrations within the fluid phase. Molecular diffusion is significant in low groundwater flow environments.

Overtopping

Inundation that occurs when the sea level exceeds the land surface elevation.

Physical groundwater model

A common form of physical model is the sand-tank, which is used to visualise physical processes, albeit under highly simplified and smaller-scale conditions than encountered in the field, that are otherwise difficult to observe.

Pleistocene

A geological epoch that lasted from about 2,588,000 to 11,700 years ago.

Recharge (*W*)

The inflow of water to a groundwater system, usually in terms of infiltration through the land surface.

Reef flat plate

A hard, low-permeability substrate (i.e. sedimentary layer) on the oceanside of atoll islands that is the landward extension to the island's fringing reef flat. The reef flat plate has an elevation of approximately mean sea level, and acts to restrict the vertical movement of ground water.

Refraction

The change in direction of groundwater flow as it passes obliquely between two layers of different properties.

Sinusoidal oscillations

A regular fluctuation (e.g. in sea level) that follows a sine wave (i.e. simple harmonic motion).

Solute dispersion

See 'dispersion'.

Steady-state conditions

The equilibrium conditions that arise when the flow into an aquifer equals the flow out, and the storage in the system (i.e. the water level) no longer changes. Steady-state conditions are often obtained by running a transient model for a long time with the same stresses (i.e. time-invariant recharge and pumping) until equilibrium is reached.

Storage coefficient (*S*)

An aquifer parameter, also known as storativity that is the volume of water released from storage per unit decline in the aquifer head per unit area of the aquifer.

Thurber discontinuity

See 'Holocene-Pleistocene unconformity (HPU)'.

Transient conditions

The conditions in an aquifer involving time-varying stresses (e.g. recharge, pumping) and water levels. Transient numerical models incorporate spatially and temporally varying recharge and pumping to produce time-series of groundwater-level distributions. Transient models are used to study systems that are in a state of flux or change.

Transition zone

The region that lies between the seawater and freshwater bodies within the aquifer where the mixing of the two fluids occurs.

Transmissivity (*T*)

An aquifer property equal to the hydraulic conductivity (*K*) multiplied by the saturated thickness of the aquifer.

1. Introduction

1.1. Background

The Bonriki Inundation Vulnerability Assessment (BIVA) project is part of the Australian government's Pacific–Australia Climate Change Science and Adaptation Planning Program (PACCSAP), within the International Climate Change Adaptation Initiative. The objectives of PACCSAP are to:

- improve scientific understanding of climate change in the Pacific;
- increase awareness of climate science, impacts and adaptation options; and
- improve adaptation planning to build resilience to climate change impacts.

The BIVA project was developed by the Geoscience Division (GSD) of the Secretariat of the Pacific Community (SPC) in partnership with the Australian government and the Government of Kiribati (GoK).

1.1.1. Project objective and outcomes

The BIVA project aims to improve our understanding of the vulnerability of the Bonriki freshwater reserve to coastal hazards and climate variability and change. Improving our knowledge of risks to this freshwater resource will enable better adaptation planning by the GoK.

More specifically, the project has sought to use this knowledge to support adaptation planning through the following outcomes:

- Improved understanding and ability to model the role of reef systems in the dissipation of ocean surface waves and the generation of longer-period motions that contribute to coastal hazards.
- Improved understanding of freshwater lens systems in atoll environments with respect to seawater overtopping and infiltration, as well as current and future abstraction demands, recharge scenarios and land-use activities.
- Enhanced data to inform a risk-based approach in the design, construction and protection of the Bonriki water reserve.
- Increased knowledge provided to the GoK and the community of the risks associated with the impact of coastal hazards on freshwater resources in response to climate change, variability and sea-level rise.

1.1.2. Context

The Republic of Kiribati is located in the Central Pacific and comprises 33 atolls in three principal island groups. The islands are scattered within an area of about 5 million square kilometres. The BIVA project focuses on the Kiribati National Water Reserve of Bonriki. Bonriki is located on Tarawa atoll within the Gilbert group of islands in Western Kiribati (Fig. 1). South Tarawa is the main urban area in Kiribati, with the 2010 census recording 50,182 people of the more than 103,058 total population (KNSO and SPC 2012). Impacts to the Bonriki water resource from climate change, inundation, abstraction and other anthropogenic influences have potential for severe impacts on people's livelihood of South Tarawa. The Bonriki water reserve is used as the primary raw water

supply for the Public Utilities Board (PUB) reticulated water system. PUB water is the source of potable water use by at least 67% of the more than 50,182 people of South Tarawa (KNSO and SPC 2012). Key infrastructure including the PUB Water Treatment Plant and Bonriki International Airport and residential houses are also located on Bonriki, above the freshwater lens, making it an important economic, social and cultural area for the Republic of Kiribati.

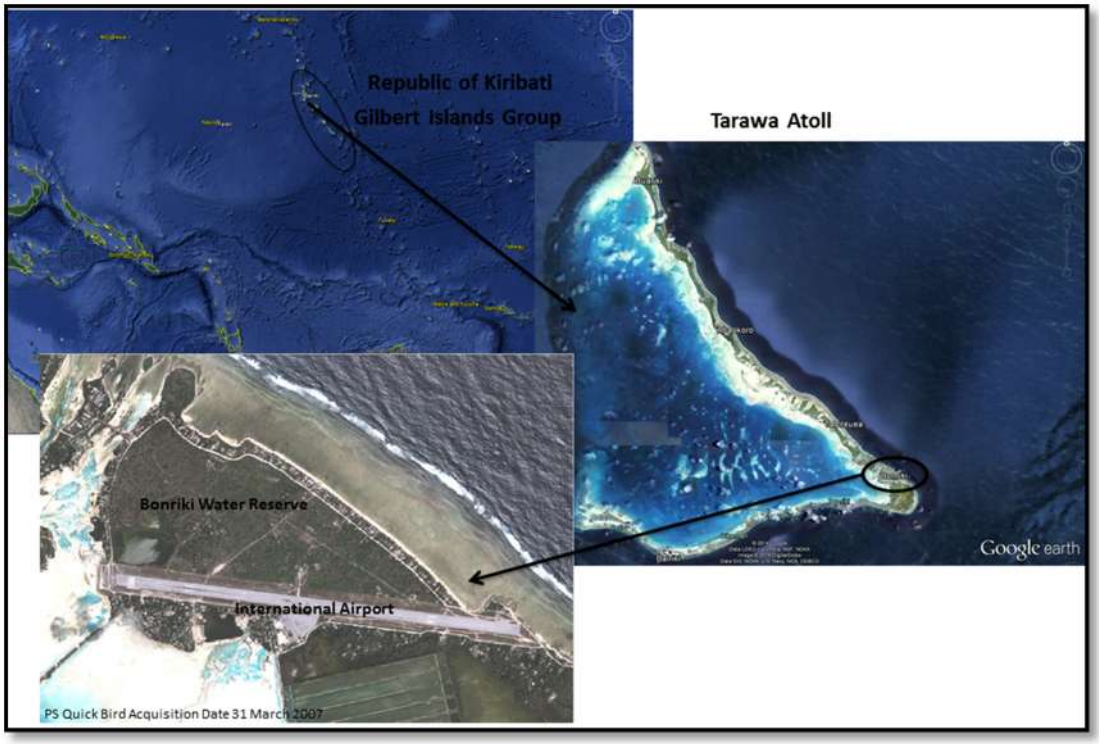

Figure 1. *Bonriki Water Reserve Location*

1.2. Purpose of this report

As illustrated in Figure 2, the BIVA project consisted of three interlinked components: stakeholder engagement, groundwater investigations and analysis, and coastal investigations and analysis. The groundwater investigations and analysis component of the project has been undertaken in a number of steps leading towards the development of a groundwater model which ultimately informs better water resource management. The purpose of this literature review was to collate and understand important information on the processes related to the occurrence of fresh groundwater lenses (FGLs) on atoll islands. Understanding these processes is a key factor in responding effectively to current and future stresses on small island water resources. In particular, an important feature of FGLs on small islands is the transition or mixing zone between fresh water and sea water. A proper characterisation of the position and thickness of the mixing zone is important for the effective management of coastal water resources (Werner et al. 2013a). Relationships between the behaviour of the mixing zone and other processes occurring on atoll islands are generally poorly defined, and have received little attention in previous literature on FGLs on atoll islands.

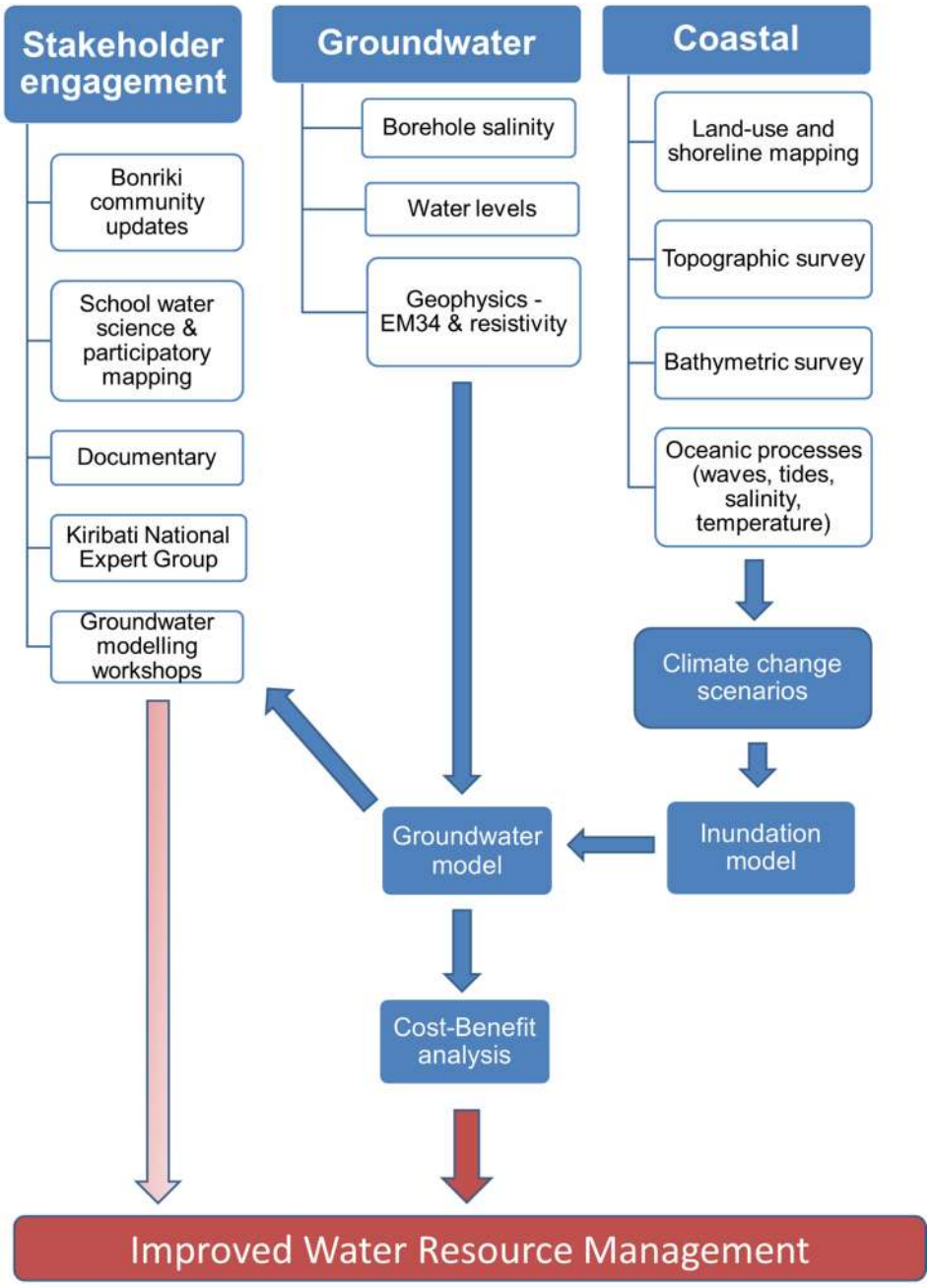

Figure 2. *Bonriki Inundation Vulnerability Assessment project components*

1.3. Scope of this report

As a preliminary component of the BIVA project, a literature review is required to document the available and background literature on Pacific atoll groundwater systems and their inundation for future guidance and reference. In particular, the literature review is intended to cover the following topics:

- General hydrogeologic and hydrologic concepts on atoll environments in the Pacific,
- Modelling groundwater systems of atolls,
- Inundation by wave overtopping of atolls fresh groundwater resources, including concepts and specific studies of such events globally.

To meet this requirement, the current document aims to review previous literature on FGLs on atoll islands, their investigation using models, and the susceptibility of these systems to impacts from ocean overtopping. In particular, we outline current knowledge gaps pertaining to the associated density-dependent flow and transport processes, and other areas of future research that are needed to improve our current understanding of these important natural resources.

2. Physical characteristics of atoll island aquifers

Atolls islands are low-lying reef carbonate islands. They usually consist of a series of narrow islands surrounding a relatively shallow seawater lagoon. Of the 425 atolls of the world, most are located in the Pacific and Indian oceans (Falkland 1991; 1992a). The maximum elevations of atoll islands are typically between 2 m and 3 m above sea level, and their dimensions vary between 100 m and 1,500 m in width, and up to several thousand metres in length (Bailey et al. 2008). The land area of most atolls is less than 1 km^2, and the width is less than 1,000 m (White and Falkland 2010). The surface area of atoll lagoons varies between 2 km^2 and 1,000 km^2, and the lagoon is generally shallow, having a depth of up to 100 m (Bailey et al, 2008).

The common structure of an atoll island consists of unconsolidated sediments (e.g. Holocene sand and gravel) that have been deposited unconformably above Pleistocene reef deposits (White and Falkland 2010), which formed on top of submerged volcanic foundations (Vacher 1997) (Fig. 3). The geological development of atolls has been explained by Darwin's evolutionary sequence of reefs (Falkland 1991; Vacher 1997), whereby subsequent to the formation of a volcanic island (Fig. 3a), the volcanic core begins to subside and the island is bordered by a 'fringing reef' (Fig. 3b). The process continues until the volcanic rocks are buried by the Pleistocene reef (Fig. 3c). Finally, Holocene deposits form the islands that surround a central lagoon in a ring-like structure (Fig. 3d). Even though the ring-like structure is typical of most atolls, there are some variations. For example, at Christmas Island (i.e. locally known as Kiritimati), the lagoon is filled and the Pleistocene limestone is exposed (Vacher 1997).

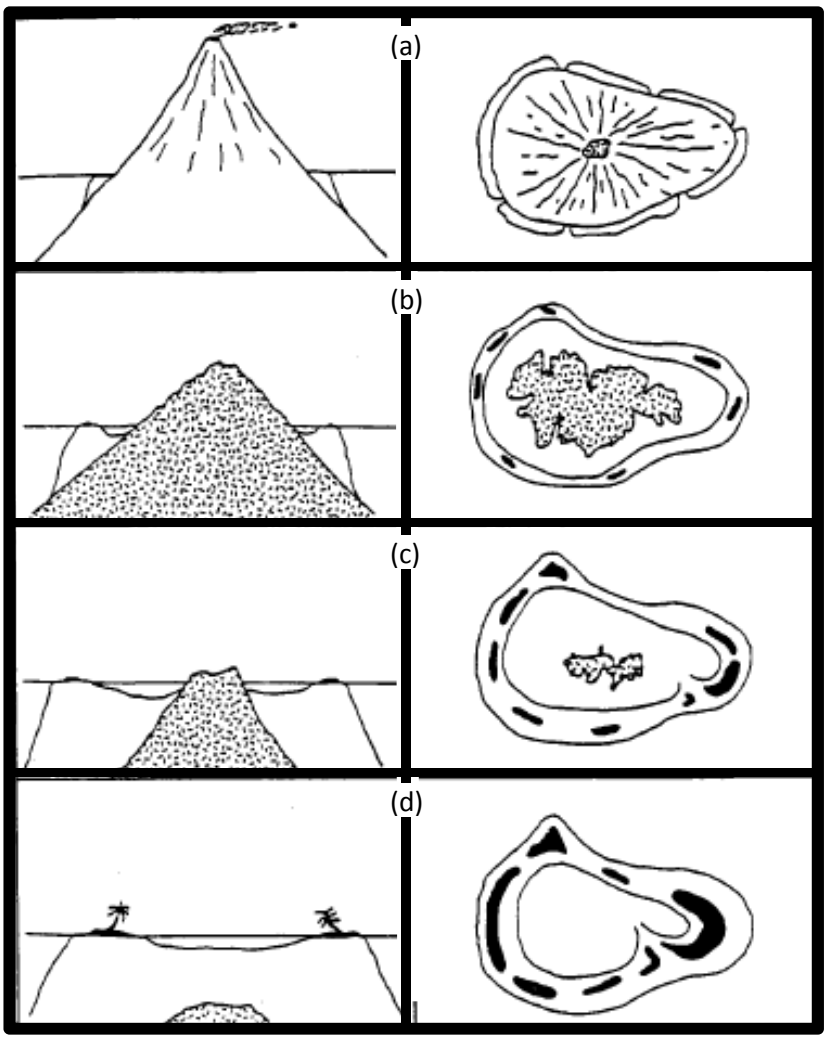

Figure 3. *Stages in the geological history of an atoll: (a) volcanic island formation, (b) and (c) subsidence of the volcanic core and fringing reef formation, and (d) final stage ring-like structure (adapted from Falkland 1991).*

In geological terms, atolls were formed in relatively recent times. While the underlying reef deposits have been dated to the final Pleistocene period, the upper layers were deposited during the Holocene period (Vacher 1997). Radiocarbon dating of the Holocene sediments indicates that prolific reef growth occurred around 8,000 years ago (Woodroffe and Falkland 1997). According to Woodroffe (2008), atoll ridges similar to modern forms existed when sea level was high during the final Pleistocene period. The reef platform was exposed during glaciations when sea level was lower, leading to extensive karstfication. Sea level rose during the post-glacial period and flooded the reef platforms around 8,000 years ago, when reef growth re-established.

The Pleistocene and Holocene deposits are very heterogeneous on atoll islands (e.g. Buddemeier and Oberdorfer 1986). According to Falkland (1991), during the final Pleistocene and during some Holocene periods, karstification processes occurred, especially during the emergence of reef sediments (Figs. 3b and 3c). The younger upper sediments are moderately permeable soon after deposition, and become gradually cemented, harder and karstified with time. These processes increase the permeability and heterogeneity of the deposits due to the development of secondary permeability by the formation of fissures (Falkland 1991). On Enjebi Island (Enewetak Atoll, Marshall Islands), the heterogeneity of reef deposits presents as short-range vertical and horizontal variations

in lithology, and through the occurrence of several solution unconformities (Buddemeier and Oberdorfer 1986). Specifically, there are significant variations in texture, lithification degree, and the occurrence of large voids and karst conduits. On Tarawa Atoll (Kiribati), Marshall and Jacobson (1985) found that the sediment heterogeneities are compounded by facies changes between corals and unconsolidated sediments along the margins of the atoll that did not develop synchronously during the Holocene. Furthermore, variability in sediment deposition was encountered across the island because finer sediments are deposited on the lagoon side, while coarse sediments are deposited on the ocean side (Falkland 1991). This was also observed by Weber and Woodhead (1972), who found that open ocean processes deposit coarse-grained sediments with a higher degree of roundness compared with the medium sediments of the lagoon. This characteristic was also reported by Ayers and Vacher (1986) for Pingelap Atoll (Federated States of Micronesia), where the hydraulic conductivity (*K*) of the Holocene sediments is higher, by one order of magnitude, in the sediments bordering the ocean compared with the sediments adjacent to the lagoon.

The Holocene–Pleistocene layering of atoll islands is often treated as a dual-aquifer system (Vacher 1997; Woodroffe 2008; Fig. 4) because of the clear demarcation and distinct differences in hydraulic properties between the two sediment types. The Holocene sediments commonly have lower *K* values relative to the karstified Pleistocene deposits (Vacher 1997). The contact between the Holocene and the Pleistocene aquifers, also known as the 'Thurber discontinuity' (Buddemeier and Oberdorfer 1997), typically occurs between 15 m and 25 m below sea level (Ayers and Vacher 1986; Falkland 1991; Bailey et al. 2008). The difference in *K* between the two layers is commonly around two orders of magnitude, with values of 1–10 m/d for the unconsolidated Holocene sediments (K_U), and 100–1,000 m/d for karst Pleistocene limestone (K_B) (Vacher 1997). An additional factor in the dual-aquifer models of many atolls is the reef flat plate, which is a semi-permeable reef rock that forms on top of the Holocene aquifer (Fig. 4). Stoddart and Cann (1965) reported that beach rock is typically developed on detrital reef islands, which are generally small, low, narrow and composed of highly permeable material. They found that beach rock from atolls in British Honduras was cemented by aragonite rather than calcite. The reef flats were formed once the reef growth caught up with post-glacial sea-level rise (Woodroffe 2008). As the sea level rose during the early Holocene period, the growing reef became exposed at ambient low-tide levels, and lateral progradation of the reef occurred (Woodroffe 2008). Where the reef flat plate exists, it acts as a confining unit, and its presence can affect the thickness and volume of FGLs (Ayers and Vacher 1986; Bailey et al. 2008).

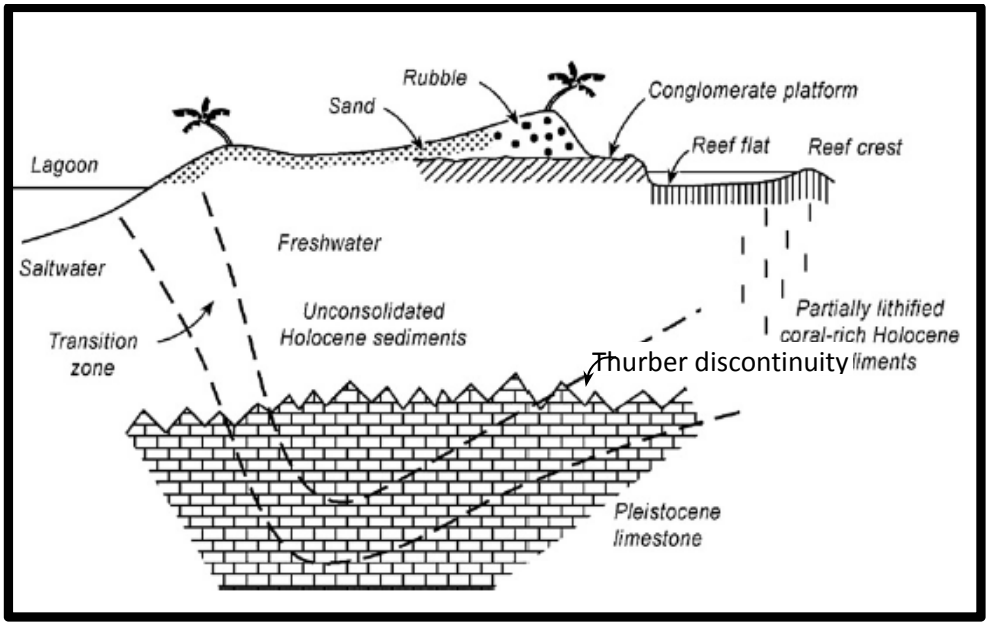

Figure 4. *Schematic representation of a fresh groundwater lens in a dual-aquifer system of an atoll island (modified from Woodroffe 2008)*

3. Hydrology and hydrogeology of atoll islands

3.1. General characteristics of fresh groundwater lenses

On small islands, when rainwater infiltration is sufficient, fresh groundwater lenses (FGLs) are formed that float above higher salinity groundwater, derived from seawater. The thickness of FGLs is usually defined as the depth below the water table to a certain salinity value. For example, Ritzi et al. (2001) adopted 50% of sea water (e.g. total dissolved salt [TDS] content of 17,500 mg/L or electrical conductivity [EC] of 25,000 μS/cm) as an approximation of the centre of the mixing zone, and to compare with sharp-interface analyses of the mixing zone position. Sharp-interface approximations apply a binary water-type approach, whereby sea water and fresh water are separated by a surface of pressure equivalence (representing the pressure imposed by the ocean) (e.g. Werner et al. 2012). Underwood et al. (1992) adopted 2.5% of sea water (approximately 500 mg/L TDS or EC of 1,250 μS/cm) to define the FGL's potable water extent, commensurate with the limit of usable or drinking water. In the Pacific, an upper limit of 2,500 μS/cm, 5% of sea water, is often adopted in defining the freshwater resource potential (Falkland and Woodroffe 1997). In reality, the lower boundary of the FGL occurs as a transition zone between freshwater and seawater, where the water salinity gradually increases from freshwater to seawater (Falkland 1992b; White and Falkland 2010).

Atoll FGLs are usually influenced by the islands' layered stratigraphic units. For example, flow lines are refracted when meteoric water, flowing from the interior of the island to the shoreline, crosses the Thurber discontinuity. We refer to the Thurber discontinuity as the Holocene–Pleistocene unconformity (HPU) is what follows. Refraction of groundwater flow across the HPU occurs due to differences in the *K* values between the two sequences (Vacher 1997). Refraction is shown diagrammatically in Figure 5.

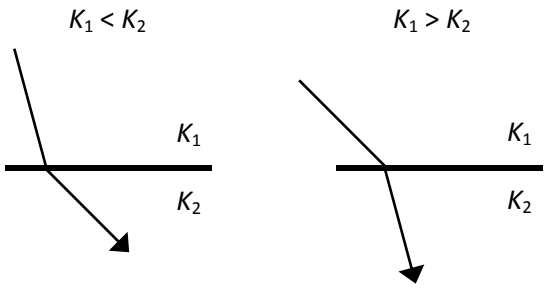

Figure 5. *Refraction of a groundwater flow line.*

The hydraulic gradients within Pleistocene layers are flatter due to the higher *K* of the karst limestone, and this causes thinning of FGLs, which tend to be truncated at the HPU (Bailey et al. 2009; Ketabchi et al. 2014). The degree of truncation at the HPU is enhanced with increasing K_B/K_U ratios, as demonstrated by Ketabchi et al. (2014) from numerical and analytical modelling. FGL truncation at the HPU has been reported for Tarawa (Kiribati; Falkland and Woodroffe 1997), at the Laura area on Majuro Atoll (Marshall Islands; Peterson 1997), in atolls of the Cocos Islands (Woodroffe and Falkland 1997), and at Diego Garcia Atoll (United Kingdom; Hunt 1997). A simple schematic of FGL truncation at the HPU is illustrated in Figure 6.

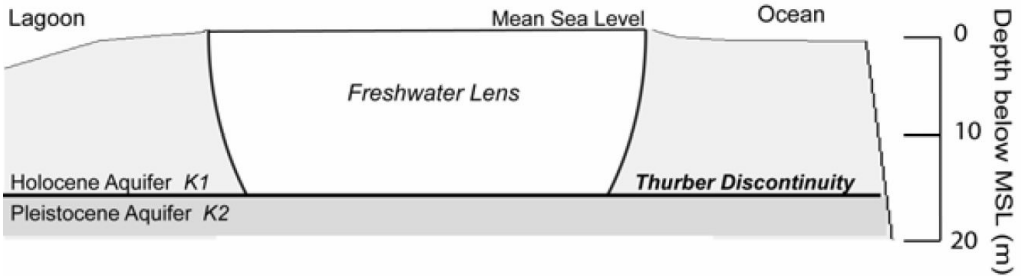

Figure 6. *Schematic of the truncation of the FGL by the HPU (i.e. the Thurber discontinuity; taken from Bailey et al. 2010).*

The factors that influence the thickness of FGLs in dual-layer aquifers of atoll islands were investigated by Underwood et al. (1992). They found that the depth to groundwater salinities of 50%-seawater (often compared with estimates from sharp-interface methods), was most sensitive to recharge, the island's width, and the Holocene layer horizontal *K.* For a high recharge rate of 2,000 mm/y, the minimum viable island width to develop a 2 m thickness FGL, was about 250 m. The minimum island width extended to 750 m for a lower recharge rate of 250 mm/y. Underwood et al. (1992) found that the depth to salinities of 2.5% of seawater (often considered as the limit of potable water) was sensitive to recharge, the Holocene layer horizontal *K*, and the degree of solute dispersion (i.e. which controls the width of the freshwater–seawater mixing zone).

In many atoll island aquifers, significant asymmetry in the shape of FGLs has been observed, attributable to heterogeneities, spatial variability in recharge, and tidal effects. For example, the lateral gradation in the grain size of sediments that typically occurs in the transverse direction to the island's main axis (i.e. coarse to fine from the ocean to the lagoon, respectively) induces hydraulic

differences, leading to lens asymmetry (Falkland, 1992a; Buddemeier and Oberdorfer 1997; Falkland and Woodroffe 1997; Schneider and Kruse 2003). Vacher (1988) studied the FGLs of strip islands (long narrow ribbon-like islands and atolls) for cases with lateral variability in recharge (W) and hydraulic conductivity (K), and concluded that differences in K can cause stronger asymmetry in the lens shape than variability in W. In the case of the Bonriki lens on Tarawa Atoll (Kiribati), the FGL is displaced towards the lagoon (Falkland and Woodroffe 1997). The asymmetry in this case has been associated, at least partly, with the variability in W between the ocean and the lagoon. Buddemeier and Oberdorfer (1986) found that lens asymmetry can also occur due to hydraulic head inequalities between the reef platform on the ocean side and the lagoon.

3.2. The freshwater–seawater transition zone

The transition (or mixing) zone that separates freshwater and seawater in atolls is an important feature of the system because it influences the depth at which potable water can be obtained. Where broad transition zones occur, there may be considerable brackish water in the aquifer, but little usable freshwater, whereas thin transition zones may allow for reasonable freshwater supplies despite conditions that might otherwise provide only a thin freshwater body. The transition zone also plays an important role in recirculating sea water within the atoll subsurface. Seawater recirculation occurs because diluted seawater returns to the sea with discharging freshwater, and this discharge of salt from the aquifer is compensated by inflowing seawater, resulting in a convection cell. Cooper (1964) examined seawater recirculation in continental aquifers, and showed that the dispersive processes that create the transition zone, in combination with the influence of the density difference between seawater and freshwater, drive the recirculation of salt water (Fig. 7). The current understanding of seawater recirculation under FGLs is less developed than continental aquifer settings.

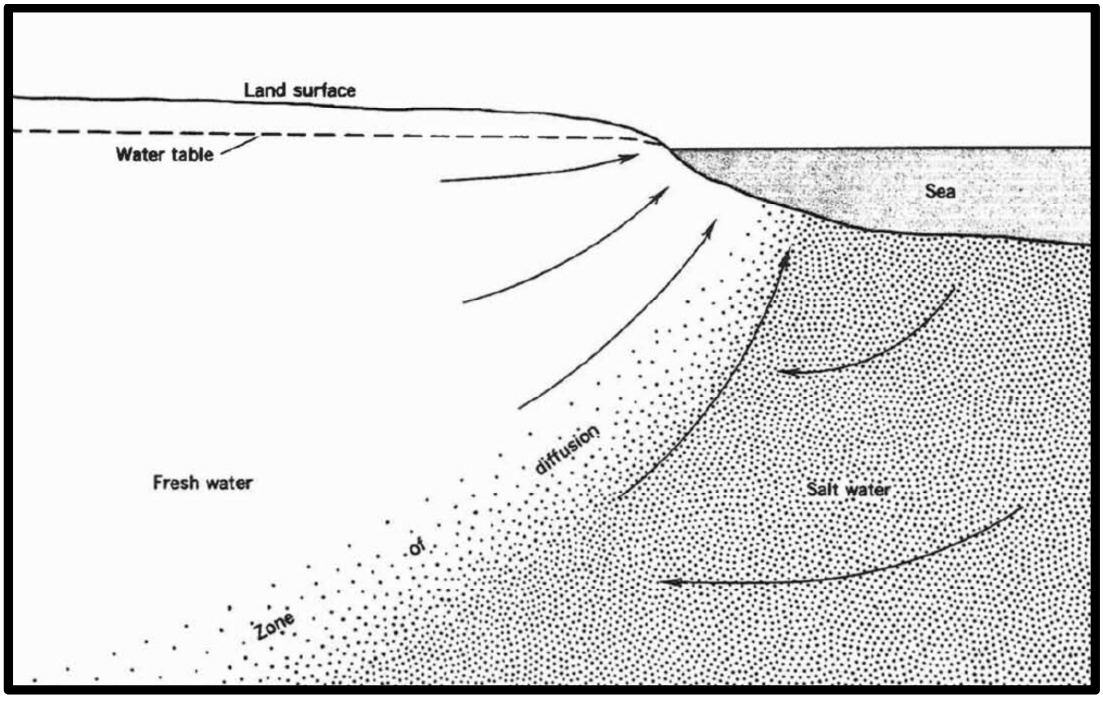

Figure 7. *Vertical cross section of a coastal aquifer showing seawater recirculation (taken from Cooper 1964).*

The transition zone is controlled by several factors, which include molecular diffusion and mechanical dispersion (Custodio and Bruggeman 1987). The latter is the macro-scale result of micro-scale heterogeneities in aquifer properties. Heterogeneity effects, more generally, influence the transition zone and the penetration of seawater into coastal aquifers, as shown by Kerrou and Renard (2010). Layered aquifer heterogeneities, such as those encountered on atoll islands, cause refraction of flow lines and this may have a profound influence on the transition zone. Lu et al. (2013) studied layering effects by considering *K* stratification and its control on the transition zone thickness. The results show that when streamlines penetrate from a high-*K* layer into a low-*K* layer, the mixing zone is widened in the low-*K* layer, and when streamlines penetrate from a low-*K* layer into a high-*K* layer, the mixing zone narrows in the high-*K* layer (Lu et al. 2013). The effect of geological layering on transition zones depends on the *K* contrast between layers, layer thicknesses, head gradients, flow directions and dispersion parameters. To date, geological stratification effects on transition zone widths have not been systematically evaluated for cases of atoll islands composed of dual-layer, Holocene-Pleistocene arrangements.

Other factors that impact the transition zone include kinetic mass transfer effects and the transience of forcing functions such as tides and recharge seasonality (Werner et al. 2013a). Kinetic mass transfer refers to solute exchange between mobile and relatively immobile zones; the latter occurs as low permeability zones and dead-end pores (Lu et al. 2009). The influence of tides on transition zones on atoll islands depends on the dual-layer arrangement and the HPU because tides propagate and attenuate at different rates through the Holocene and Pleistocene sediments, creating a complex arrangement of tidally driven hydraulic head fluctuations. These are known to have a significant bearing on the thickness of the transition zone (Vacher 1997).

The exact nature and contribution of the different factors that affect the thickness of the transition zone, for both continental and island aquifers, are not completely understood (Werner et al. 2013a). As such, studies of freshwater availability need to explore the contributions of various factors that may modify the salinity distribution on atoll islands because ignoring certain factors that potentially modify the mixing zone may result in inaccurate estimation of fresh ground water. For example, neglecting mixing processes and assuming a sharp freshwater–seawater interface may lead to a significant overestimation of freshwater resources within the atoll aquifer (Oberdorfer et al. 1990).

Figure 8 shows four different cases of islands in which the transition zone is affected by different factors. In the Bonriki lens of Tarawa Atoll (Fig. 8a; Falkland and Woodroffe 1997), the upper half of the transition zone, defined by electrical conductivities between 2,500 µS $cm^{-1}$and 25,000 µS cm^{-1}, is thicker towards the ocean side, and thinner in the centre of the island. Across Bermuda, the thickness of transition zones, defined by salinities between 1% and 99% of sea water, show geologic control (Fig. 8b; Vacher and Rowe 1997). The transition zone of Nauru Island is also variable, although the same asymmetry is not present as observed elsewhere (Fig. 8c; Ghassemi et al. 1996). Significant asymmetry is evident in the transition zone of Enjebi Island, Enewetak Atoll, leading to only minor thicknesses of fresh water (Fig. 8d; Buddemeier and Oberdorfer 1997). The combined effects of geology, recharge variability, tidal mixing, pumping, ocean overtopping and boundary condition effects that lead to asymmetry in transition zones have not been properly explored on atoll islands, at least in a general sense.

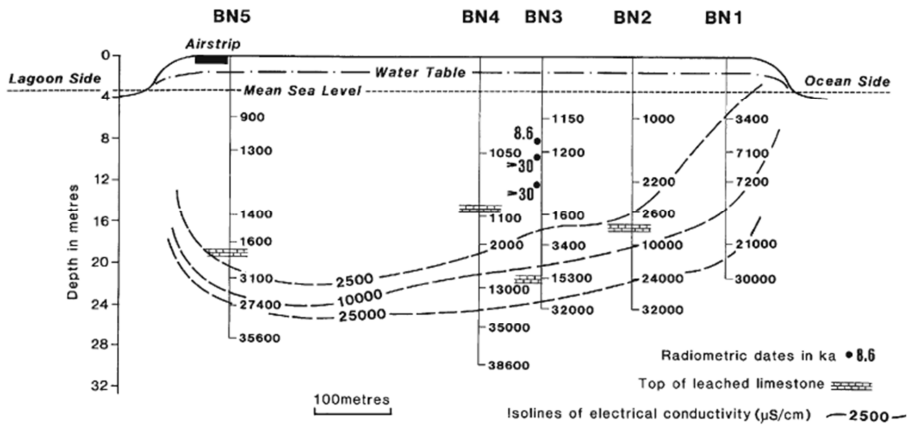

(a) Cross section of Bonriki, Tarawa Atoll (Kiribati). Contours show groundwater electrical conductivity [µS cm^{-1}] (taken from White and Falkland 2010).

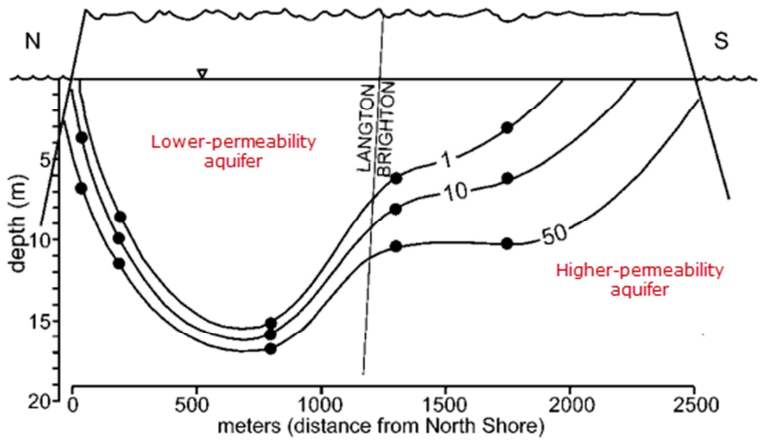

(b) Cross section in the central lens of Bermuda. Contours show relative salinity as % of seawater (taken from Vacher and Rowe 1997).

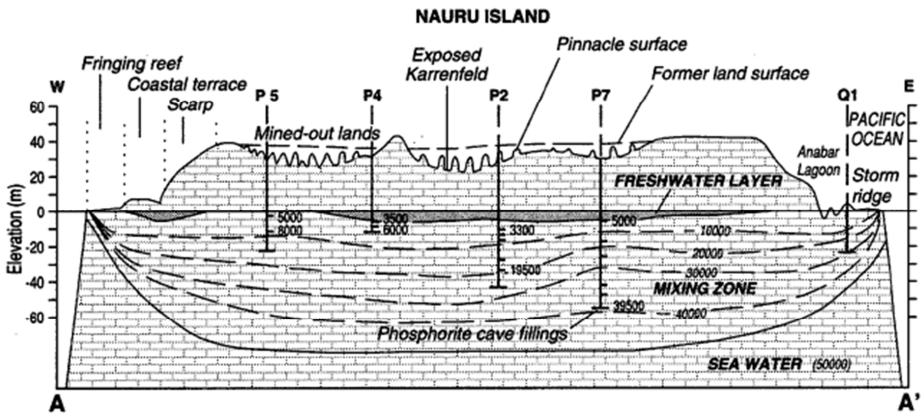

(c) Cross section of Nauru Island. Contours show groundwater electrical conductivity [µS cm^{-1}] (taken from Ghassemi et al. 1996).

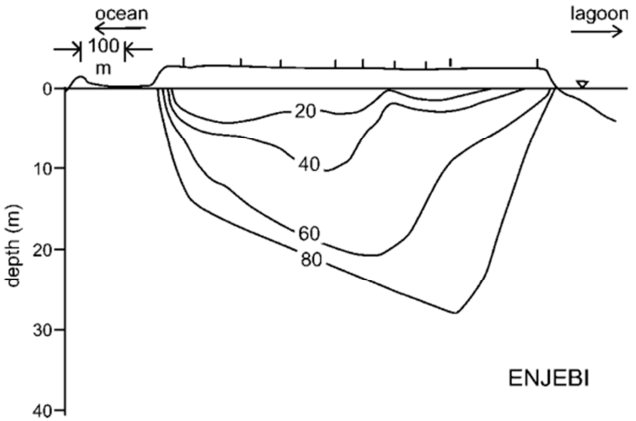

(d) Cross section of Enjebi Island, Enewetak Atoll. Contours show the average location of salinity as % of sea water (taken from Buddemeier and Oberdorfer 1997).

Figure 8. *Cross sections showing across-island variations in thicknesses of fresh ground water and widths of transition zones: (a) Bonriki, Tarawa Atoll, (b) Bermuda limestone islands, (c) Nauru Island, raised coral atoll, and (d) Enjebi Island, Enewetak Atoll.*

In some atoll islands, mixtures of freshwater and seawater can be found at considerable depths. Case studies of islands with dual-aquifer model configurations have shown that the transition zone, between 2.5% and 95% of seawater concentration, may occupy a considerably greater volume of the aquifer compared to the freshwater component (i.e. <2.5% of seawater concentration) (Buddemeier and Oberdorfer 1986; Ghassemi et al. 1996; Buddemeier and Oberdorfer 1997; Jacobson et al. 1997). For example, on Nauru Island, the Holocene deposits have risen and dried out the lagoon, allowing the formation of a thin freshwater lens up to 7 m thick in the limestone Pliestocene aquifer that overlays a mixing zone of brackish water up to 60 m depth (Fig. 8c). On Enjebi Island, Enewetak Atoll, fresh water occurs through only a few metres below the water table due to extensive brackish transition zones (up to 80 m depth) (Fig. 8d). Buddemeier and Oberdorfer (1997) found that on Enjebi Island, salinity profiles seem to be correlated with the location of solution unconformities, and are independent of tides and seasons.

3.3. Tidal effects

In coastal aquifers, groundwater flow patterns, salinity distribution, and the location of water flow across the land–sea boundary are influenced by tides (Werner and Lockington 2006; Mulligan et al. 2011; Post 2011). In atoll islands, the water levels of both the ocean and the lagoon fluctuate with the tide, forcing the aquifer water level to fluctuate at reduced amplitude and with a time delay or lag (Hunt and Peterson 1980). The tidal lag is the time difference between the ocean high tide and high tide at a particular location in the aquifer. The reduction in amplitude is quantified by the tidal efficiency, which is the ratio of groundwater level fluctuation to that of the ocean. For example, if a groundwater tidal amplitude of 0.75 m arises from a spring ocean tide of amplitude equal to 1.5 m, the tidal efficiency is 0.75/1.5 x 100% = 50%. Note that the tidal amplitude is the height of high tide above mean sea level, or half the height difference of high tide minus low tide.

The dampening or attenuation of tidal signals in coastal aquifers is caused by the friction associated with the movement of water through the pore spaces of the island and seafloor sediments. Hence, the composition and hydraulic properties of the aquifer material determine the efficiency with which the tidal pulse is transmitted. Higher tidal efficiencies and shorter time lags indicate greater 'hydraulic connectivity' of the aquifer to the ocean and/or lagoon. The propagation and attenuation of tidal oscillations in coastal aquifers that lead to groundwater head fluctuations were evaluated by Ferris (1951). He showed that in a confined, homogeneous aquifer, sinusoidal oscillations in pressure will propagate along the aquifer according to:

$$h = Ae^{\left(-x\sqrt{\frac{\pi S}{t_0 T}}\right)} \sin\left(\frac{2\pi t}{t_0} - x\sqrt{\frac{\pi S}{t_0 T}}\right) \quad (1)$$

Where h is the groundwater head relative to mean sea level (L), x is the distance from the sea (L), t is time (T), t_0 is the period of tidal oscillation (T), A is the amplitude of the tidal oscillation (L), T is the transmissivity of the aquifer (L^2T^{-1}), and S is the storage coefficient of the aquifer (-). According to equation (1), tidal amplitude decreases exponentially with distance from the coast. This is known as the tidal efficiency (ε), and is given by:

$$\varepsilon = e^{\left(-x\sqrt{\frac{\pi S}{t_0 T}}\right)} \quad (2)$$

The tidal oscillation propagates through the aquifer with a time lag that increases with distance from the coast. The time lag factor t_τ is given as (Ferris 1951):

$$t_\tau = x\sqrt{\frac{t_0 S}{4\pi T}} \quad (3)$$

The equations of Ferris (1951) indicate that tidal efficiency is greater and the time lag is shorter in aquifers with higher *T* and lower *S.* For unconfined aquifers, this theory can be applied when the tidal amplitude is a small fraction of the saturated thickness (Ferris 1951), and the transmissivity can be assumed constant. Equations (2) and (3) are used routinely to estimate aquifer properties *T* and *S* from the characteristics of tidally driven groundwater oscillations.

Equations (2) and (3) offer useful insights into the propagation of tides into homogeneous coastal aquifers. For situations of layered aquifers, through which the attenuation of tides will differ, complicated relationships in tidally driven head variations can arise. Underwood et al. (1992) showed that in aquifer systems comprising two layers, tidal responses (ε and t_τ) are sensitive to the contrast in *K* between the upper (K_U) and lower (K_B) layers. If K_U is significantly less than K_B (i.e. as observed in the upper Holocene and lower Pleistocene layers of many atoll islands), the tidal wave will persist further inland in the lower aquifer and subsequently propagate upwards into the upper layer from below. This will present in field situations as an increasing value of ε with depth, while t_τ will decrease with depth. In some cases, the complex geological arrangements of atoll islands produce ε and t_τ values from groundwater head analyses that appear to be virtually independent of the horizontal distance to the shore (Oberdorfer et al. 1990; Peterson 1997; White and Falkland, 2010). This occurs because tidal fluctuations propagate easily through the highly conductive Pleistocene layer, subsequently travelling upwards to modify the water level behaviour of the Holocene sediments (Underwood et al. 1992; White and Falkland 2010) (e.g. Fig. 9).

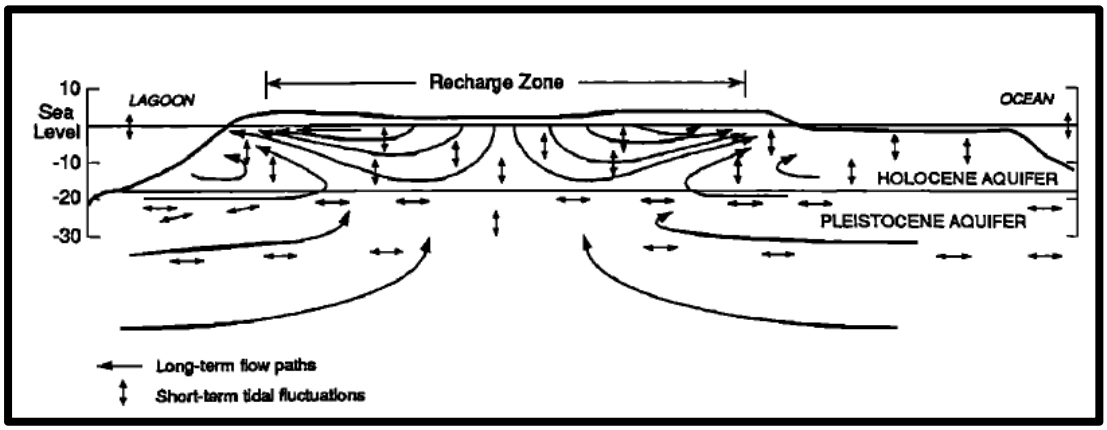

Figure 9*. Mean groundwater flow lines and tidal fluctuations under an atoll island (taken from Underwood et al. 1992).*

According to White and Falkland (2010), typical values for tidal efficiency and lag time on islands with fine sediments are around 5% and 2.5 h, respectively, while islands with coarser sediments

have ε and t_τ values of approximately 45% and 2 h, respectively. Alam et al. (2002) reported tidal efficiencies at gallery pumping stations in the Bonriki lens of Tarawa Atoll of 4% and 6.6%, and tidal lags between 2 h and 3 h. Tidal attenuation did not show any correlation with distance to the coast. Buddemeier and Oberdorfer (1997) found ε and t_τ ranges for Enewetak Atoll of 4–33%, and 1.7–3.7 h, respectively. These variations also failed to show a coherent geographic pattern. The highly conductive Pleistocene layer of Nauru Island produces ε and t_τ values of nearly 50% and around 1.5 h, respectively (White and Falkland 2010).

An important outcome of tidal fluctuations on atoll islands is the influence on the mixing zone. The cyclic movement of ground water tends to enhance the mixing between fresh water and sea water, thereby creating wider transition zones, although quantifying the degree to which this occurs is challenging. This requires some estimation of the mixing processes occurring within the aquifer, including hydrodynamic dispersion, which relates groundwater flows to the width of the transition zone. In atoll systems with significant tidal forces, the resulting mixing of seawater and freshwater is expected to be enhanced (Underwood et al. 1992). There are complicated relationships between the geological structure of atoll islands and solute mixing. For example, tidal mixing forces may propagate vertically within the aquifer (i.e. from the Pleistocene to the Holocene layers). The effect on the transition zone between fresh water and sea water depends on dispersivity parameters (i.e. transverse and longitudinal dispersivity; Underwood et al. 1992; Abarca et al. 2007). In practice, dispersivity parameters are commonly obtained through model calibration. However, whether or not tidal fluctuations are considered, and the degree to which aquifer heterogeneities are represented, have a significant bearing on dispersivity parameters because dispersivity is typically a surrogate for the mixing processes associated with both tidal forcing and heterogeneities, among other factors. Additionally, dispersivity values are dependent on the scale of observation (e.g. Gelhar et al. 1992).

In the intertidal zone, tidal oscillations influence the flow and salinity distribution, in particular on sloping beaches, generating a seawater circulation cell in the upper nearshore aquifer (Robinson et al. 2006; Werner and Lockington 2006) (Fig. 10). This circulation of seawater results in the formation of an upper saline plume (USP) in the intertidal region. Water infiltrates the beach at the high tide mark, and exfiltrates near the low tide mark. The salinity profile in the USP shows inverse gradients, with tidally driven recirculating sea water mixing with fresh ground water as it flows towards the sea floor (Robinson et al. 2006; 2007). The USP and the lower density-driven seawater wedge are separated by a discharge tube of fresh groundwater, which commonly outflows near the low tide mark (Fig. 10). Given the wide array of chemical reactions occurring through the seawater–freshwater mixing of coastal aquifers, Moore (1999) and others refer to this zone as the subterranean estuary.

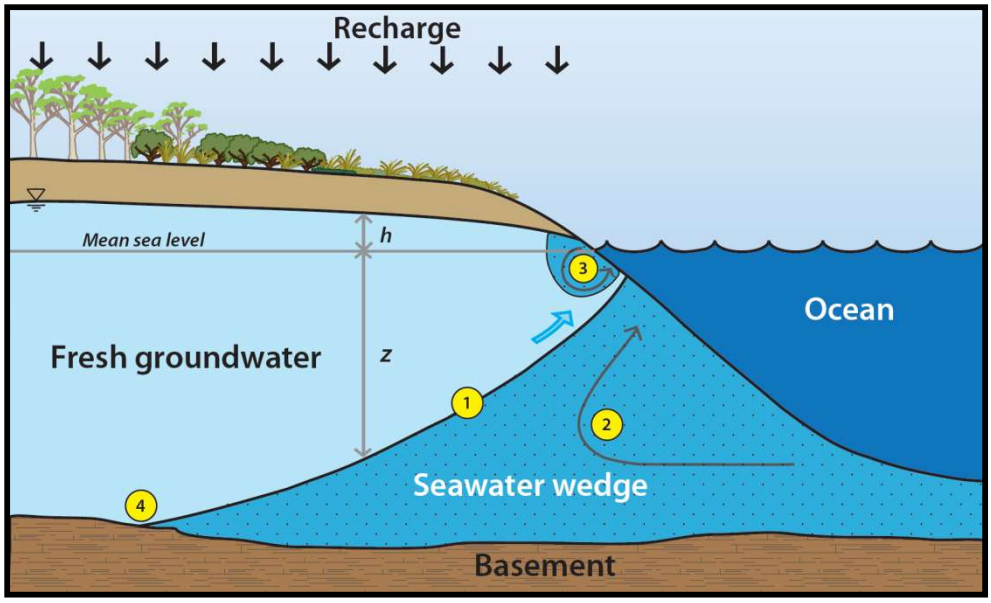

Figure 10. *Conceptualisation of the subterranean estuary in a homogeneous, unconfined aquifer: 1) the freshwater–seawater transition zone, which is a gradual transition in salinity rather than the commonly assumed sharp interface (as illustrated for simplicity); 2) density-driven circulation in the lower saline plume; 3) tide- and wave-driven upper saline plume (USP); and 4) the seawater wedge toe (Werner et al. 2013b)*

Another important aspect of tidal forcing on watertable dynamics is the development of a seepage face, which is the outcrop of ground water that develops when the tidal stage falls faster than the watertable in the aquifer (Post 2011). When the tide drops, sea level can fall more rapidly than the watertable elevation, and a decoupling occurs with the water table at the beach face higher than the sea level. The exit point corresponds to the intersection of the decoupled water table with the beach profile. The position of the exit point is independent of the tidal elevation until it is met by the rising tide (Horn 2006). Turner (1995) provided guidance on the development of seepage faces in defining the critical parameter (σ), which compares the maximum rate of tidal decline with the maximum rate of fall in the groundwater exit point, as:

$$\sigma = \frac{2\pi h_0}{t_0} \cdot \frac{n}{K \sin^2 \beta} \quad (4)$$

The maximum rate of tidal fall ($2\pi h_0/t_0$) is a function of the tidal amplitude (h_0) and the tidal period (t_0). The maximum rate of drop in the exit point ($n/K\sin^2\beta$) depends on K, porosity (n) (-), and the slope of the beach face (β). If both rates of fall are equal or the exit point is able to fall faster than the tidal rate of drop $\sigma \leq 1$, there is no seepage face development. A seepage face is expected to occur if $\sigma > 1$.

3.4. Seawater overtopping impacts on atoll islands

The low land surface elevation of atoll islands makes them vulnerable to inundation by sea water as a result of storm surges, wave setup, extremely high tides and tsunamis (Terry and Falkland 2010; Bailey and Jenson 2014). In the literature, this process is referred to as 'overwash' or 'overtopping' (see Fig. 11). Concern over the increased incidence of overtopping and the effects on freshwater lenses on low-lying atolls has increased as sea- level rise is expected to accelerate over the coming

decades (Bricker 2009). Hoeke et al. (2013) report that recent sea-level rise is contributing to the severity of recent of island inundation, and will lead to increasing inundation risks in the future.

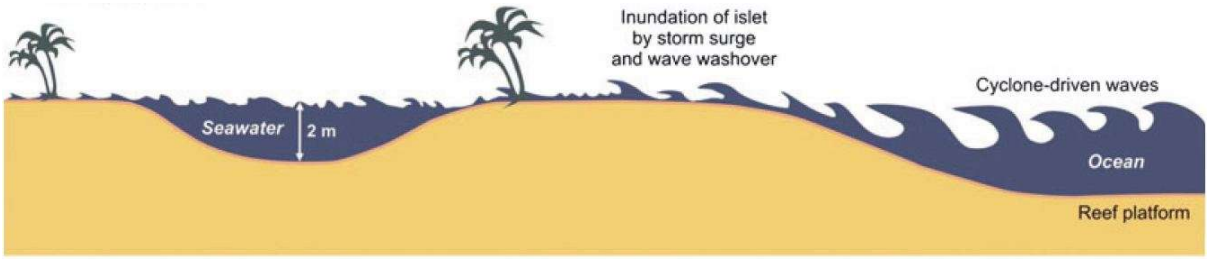

Figure 11. *Simplified conceptualisation of storm-event overwash of an atoll islet (taken from Chui and Terry 2012).*

There are a growing number of studies that investigate the effect of overtopping on the freshwater reserves of islands. While several overtopping events have been reported in the literature (Bailey and Jenson 2014), there are few direct observations that reveal the impact on groundwater salinities. Anderson and Lauer (2008) show the total dissolved solid concentration (TDS) as a function of time in the water pumped from a well field since the passage of hurricane Emily over Hatteras Island, North Carolina, USA in 1993. The values increase from less than 100 parts per million (ppm) to more than 500 ppm. Salinities increase during the first 50 days and then start decreasing to pre-hurricane levels over a period of 150 days. These values were measured in the raw water entering the treatment plant and do not provide a spatially explicit overview of the salinity distribution within the lens.

More detailed field observations are available for Pukapuka Atoll in the Northern Cook Islands where a category 5 cyclone resulted in a storm surge in February 2005 (Terry and Falkland 2010). Differences were observed between relatively shallow lenses (~ 3 m), in which the saline water was dispersed within the main body of the lens, and thicker lenses (~ 10 m), where a saline plume developed within the upper part of the lens. These saline plumes were observed to persist for several months and remnants were still observable after 26 months (Terry and Falkland 2010).

In areas that were affected by the 2004 'Boxing Day' tsunami, the presence of dug open wells was shown to be a potential pathway for sea water infiltration (Illangasekare et al. 2006). Local depressions in which sea water remained behind after the flood were also found to play a critical role in explaining the observed increase in groundwater salinities (Violette et al. 2009). One of the management responses was to try to remove the infiltrated sea water by increased pumping, but adverse effects of this approach were noted in some areas, as the salinities in the wells increased as a result of saltwater upconing (Illangasekare et al. 2006). Groundwater salinities were expected to recover to freshwater levels within a few years after the flooding occurred, but in some areas, salinities persisted longer than anticipated (Illangasekare et al. 2009), with the reasons for this remaining unclear.

Modelling studies have complemented the knowledge about overtopping effects on freshwater lenses. The study by Anderson and Lauer (2008) suggested that overtopping contributed more to the width and morphology of the freshwater–saltwater transition zone beneath Hatteras Island than

tidal oscillations due to the relatively low permeability of the island sediments and the microtidal regimes. Chui and Terry (2012) and Terry and Chui (2012) used numerical modelling to study the migration of the saline plume that penetrated the freshwater lens following an overtopping event. In the latter investigation, Terry and Chui (2012) assessed the combined effects of sea-level rise and overtopping. They found that the plume first migrates downward before discharging towards the ocean through the permeable deeper limestone layers. Their model also suggest that a low watertable elevation is more damaging to the lens than a prolonged duration of inundation, and that inundation by seawater in low-lying parts of the island caused lens recovery to be prolonged. Model parameters that tended to mitigate the effect of the overtopping event included a low anisotropy and a high vertical dispersivity. In a follow-up study, Chui and Terry (2013) suggested that the reduced thickness of the unsaturated zone that may result from sea-level rise could mitigate the adverse effects of overtopping, as a thinner unsaturated zone reduces the accumulation of saltwater in the subsurface during the inundation stage.

More recently, Bailey and Jenson (2014) focused on the influence of hydraulic conductivity, dispersion and the geological structure on salinisation by overtopping, as well as the timing of the event. They conducted a numerical modelling study of a hypothetical island using tidal and meteorological data representative for the western Pacific. Recovery times were found to be in the range of 12–16 months, but for the depths to which hand-dug wells are excavated the recovery times are less. Bailey and Jenson (2014) further concluded that reef plates, with a relatively low permeability, can act as a barrier to seawater penetration.

Currently, overtopping studies based on numerical modelling are being conducted for Andros Island in the Bahamas (Holding and Allen 2014) and for Roi-Namur island of Kwajalein Atoll, Republic of the Marshall Islands (Gingerich and Voss 2014). For the latter, salinity measurements were made during a storm surge event but they have not been published. The results of this study, which also involves the development of a numerical model, appear to be highly relevant to the Bonriki lens of Tarawa Atoll due to the numerous similarities between the two islands.

4. Modelling of atoll island aquifers

Groundwater models are a simplified representation of field situations, whereby the key features of the hydrogeological system are included to allow the modeller insights into the behaviour of the subsurface in a manner that is not possible from field observations alone. Groundwater models can be physical or mathematical. A physical model (e.g. a sand tank) provides an opportunity to visualise scaled-down groundwater processes, albeit in a highly simplified domain relative to the conditions encountered in the field. A mathematical model represents the predominant controlling processes by solving one or more of the governing equations for groundwater flow, and perhaps solute transport.

Mathematical models may be divided into analytical models and numerical models. Analytical models are applicable to highly idealised situations and require simplifying assumptions that may prove quite restrictive for many of the water resources and environmental management questions that are common for atoll islands. For example, the properties of the aquifer and the stresses on the

system (e.g. recharge and pumping) are usually considered to be constant in space and time to enable solution of a given problem.

A numerical model divides space and/or time into discrete pieces, enabling more complex, and potentially more realistic, representations of groundwater systems to be developed. Numerical models of freshwater lenses, that consider the mixing of sea water and fresh water, require representation of dispersive transport processes and the water density variations that depend on solute concentrations. Numerical models may require lengthy run times, and therefore, it is common to try to limit the number of model calculations by adopting model grids that are as coarse as possible. It is common to develop a two-dimensional vertical cross-sectional model of an atoll freshwater lens, to avoid the computation burden of three-dimensional simulation. This approach simulates only a slice of the study area, however. Three-dimensional numerical models of atoll island aquifers are less common due to their higher computing demands.

It is standard practice to develop one or more steady-state models of groundwater systems. These models apply time-invariant model stresses, and simulate the equilibrium conditions that arise under constant stresses and after a considerable period of time. Steady-state models offer useful insights into long-term average lens conditions, and are typically applied as the starting conditions for transient models, which simulate time-varying behaviour.

Model choice is determined by the type of questions that are asked, and the amount and quality of available information about the system. A modeller must decide on a model code, which is the type of software that is used to simulate groundwater flow and transport processes in the aquifer. A wide variety of codes is available, and these differ in their ability to simulate particular conditions, their user-friendliness and their cost, among other factors. However, regardless of the model used, the prediction of solute concentrations and fluxes, and groundwater heads and flows, invariably brings with it significant uncertainties. The magnitude of these depends on the available knowledge pertaining to the aquifer parameters, the representativeness of the flow and transport processes in the model relative to field conditions, the available computer power, the resources and time expended on model development, and the experience of the modelling team, among other considerations.

Approaches to evaluating atoll island aquifers can be subdivided into: 1) analytical solutions that rely on the sharp-interface approximation of the freshwater–saltwater interface and consider only steady-state conditions; and 2) numerical methods that allow for the representation of the dispersive processes that lead to transition zones between freshwater and seawater, and are able to simulate both steady-state and transient conditions. The advantages of analytical solutions are the ease of use and the limited computational requirements, whereas the benefits of numerical methods lie in their flexibility to investigate a wide range of complex situations and processes.

4.1. Analytical solutions of FGLs

Analytical solutions have been developed to describe the shape of FGLs on small islands based on the Ghyben-Herzberg (GH) approximation and the Dupuit assumption (Strack 1989). The Dupuit assumption neglects resistance to flow in the vertical direction, so that the vertical pressure distribution is hydrostatic (Werner et al. 2013a). The GH approximation considers that seawater and freshwater are immiscible, and that a line of pressure equivalence occurs between sea water and

fresh water (Custodio and Bruggeman 1987) (Fig. 10). At any point along the sharp interface, the pressure head on both sides must be the same. For example, in Figure 10, the pressure (P_A) in the freshwater zone is given by:

$$P_f = \rho_f g(h+z) \quad (5)$$

Where z is the depth to the freshwater–seawater interface below mean sea level (L), ρ_f is fresh water density (ML^{-3}), and h is the watertable elevation above mean sea level (L). The corresponding saltwater pressure is:

$$P_s = \rho_s g z \quad (6)$$

where ρ_s is seawater density (ML^{-3}). Assuming hydrostratic conditions and combining equations (5) and (6) through $P_f = P_s$, produces the GH relationship:

$$z = \frac{\rho_f}{\rho_s - \rho_f} h = \alpha h \quad (7)$$

It is common to adopt a value of 40 for α, although it can vary between 33 and 50 (Custodio and Bruggeman 1987). Fetter (1972) used the GH relationship to describe the watertable elevation for a homogeneous infinite strip and circular islands under constant distributed recharge. The expression for an infinite strip island (see Fig. 12) is given by:

$$h(x) = \sqrt{\frac{W(L^2 - x^2)}{K(1+\alpha)}} \quad (8)$$

where W is the recharge (MT^{-1}), and L is half of the island width (L).

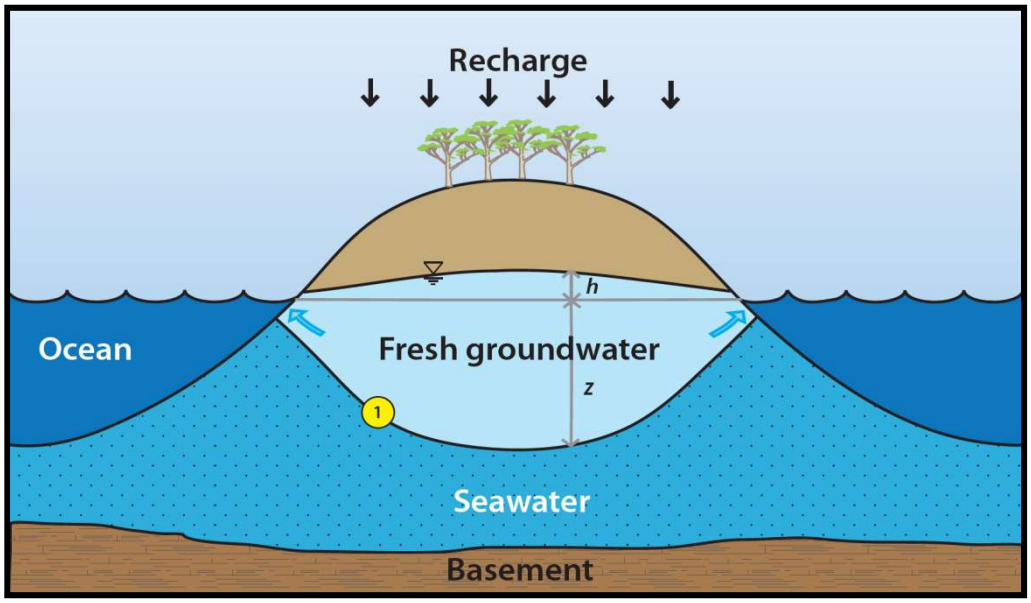

Figure 12. *Fresh groundwater lens in a homogenous strip island (Werner et al. 2013b).*

Combining equations (7) and (8) provides the location of the interface, as (Fetter 1972):

$$z(x) = \alpha \sqrt{\frac{W\left(L^2 - x^2\right)}{K\left(1+\alpha\right)}} \quad (9)$$

From equations (8) and (9), the thickness of the lens ($h + z$) is greater for higher values of the ratio W/K and for wider islands (L).

Vacher (1988) presented analytical solutions for FGL in strip islands for several arrangements of zoned differences in *K* and *W* (Fig. 13). Lateral variability in *K* and W produced asymmetry in the FGL, as expected. That is, the lens is thicker where *W* is higher, or where *K* is lower (Figs. 13b and 13c). Vacher (1988) also analysed layered systems (Figs. 13d and 13e). He found that arrangements where a high-*K* layer underlies a lower-*K* layer, and the lens reaches the high-*K* layer, the interface is refracted and the lens becomes thinner, compared with the case of a single-layer system (Fig. 13d). In essence, there is somewhat of a truncation of the lens thickness by the underlying high-*K* sequence. As expected, if the lower layer is impermeable (Fig. 13e), the lens is truncated at the contact with the basement, and the water table will be higher than situations where the aquifer extends beyond the bottom of the FGL (Vacher 1988). Ketabchi et al. (2014) extended Vacher's (1988) analytical solutions by providing solutions for layered circular islands, and they considered the effects of land-surface inundation in both strip and circular (dual-layer) islands. They demonstrated that under sea-level rise, land-surface inundation is often a more important factor than the pressure increase of the rising sea in terms of impacts on the FGL. Morgan and Werner (2014) also extended the work of Vacher (1988) by developing seawater intrusion vulnerability indicators, based on derivatives of analytical solutions as undertaken previously for continental aquifers by Werner et al. (2012). Their method provides a formal basis for ranking the susceptibility of strip island FGLs to impacts from recharge change or sea-level, considering land-surface inundation and both flux-controlled and head-controlled inland boundary conditions, as defined previously by Werner and Simmons (2009).

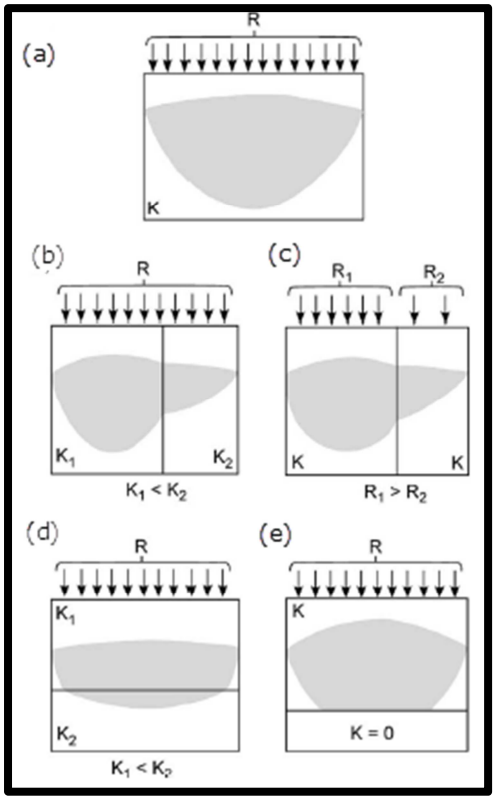

Figure 13. *Fresh groundwater lens (FGL) conceptual models of FGLs analysed by Vacher (1998): (a) Homogeneous R and K, (b) Variable K, (c) Variable R, (d) dual-aquifer system with a high-K bottom layer, (e) Impermeable layer at the bottom (taken from Schneider and Kruse 2003).*

One of the consequences of using the Dupuit assumption in developing FGL analytical solutions is that the ocean boundary condition is one where the water table and the interface meet at the shoreline, whereas in reality, a subsurface outflow face is expected that allows for the discharge of fresh groundwater to the sea (Fig. 14; Fetter 1972; Vacher 1988). Glover (1959) developed the first solution, using flow net analysis and otherwise adopting similar assumptions as required for the GH approximation, for the position of the interface at the shoreline that accounts for the presence of the outflow face. The vertical depth to the interface at the shoreline (y_0) is the simple function $y_0 = Q\alpha/K$, where Q is discharge to the sea (L^3T^{-1}). The offshore extent of the outflow face (x_0) is given by $x_0 = y_0/2$ (Glover 1959). Extensions to Glover's (1959) outflow face solutions were developed by Van der Veer (1977). According to Vacher (1988), the effect of the outflow face is negligible, except for a narrow fringe adjacent to the shoreline, accounting for about 1–5% of the width of the island.

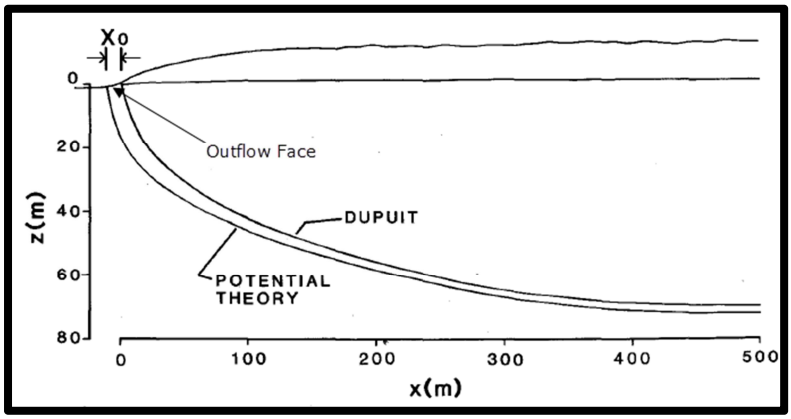

Figure 14. *Comparison of the position of the interface given by Dupuit analysis and potential theory for fresh groundwater lens (taken from Vacher 1988).*

Volker et al. (1985) developed an analytical solution for the thickness of the mixing zone of a strip island. The mixing zone was superimposed over the sharp-interface approximation of the transition zone, based on assumptions of steady-state, horizontal flow in a homogeneous aquifer receiving

variable zones of surface recharge. The authors treat the transition zone as a boundary layer of finite width, above and beneath which the fluid properties change to fresh water and sea water, respectively. The steady-state thickness of the transition zone (δ) is given by:

$$\delta = \lambda^{-1/2} R_0 \frac{\left(L^2 - x^2\right)^{1/2}}{x}\left[1 - \left(\frac{L^2 - x^2}{L^2}\right)^{1/2}\right]^{1/2} \quad (10)$$

Where R_0 (L) is the radius of curvature of the interface at the centre of the symmetric island, which can be estimated, based on the GH approximation, as (Volker et al. 1985):

$$R_0 = \frac{L}{\sqrt{\frac{\alpha W}{K\left(1 + \frac{1}{\alpha}\right)}}} \quad (11)$$

The Rayleigh number λ [-] is given by $KR_0/D\alpha$ (Volker et al. 1985), where D is the dispersion coefficient (L^2T^{-1}), which was assumed homogeneous and isotropic. Given that mechanical dispersion is velocity dependent, this assumption may have limited application. The expressions developed by Volker et al. (1985) imply that the thickness of the transition zone is maximum at x = 0, and decreases towards the island's edge. However, the model cannot predict δ accurately near the shoreline (i.e. x is close to L), because the horizontal flow and homogeneous, isotropic D assumptions do not hold in this area (Volker et al. 1985).

Using the Volker et al. (1985) model, White and Falkland (2010) produced an expression to represent the ratio of the transition zone thickness δ to the freshwater lens thickness H_U, at the centre of the lens, as:

$$\frac{\delta}{H_U} = \frac{K}{W}\left(\frac{\alpha D}{2LK}\right)^{1/2} \quad (12)$$

According to equation (12), the relative thickness of the transition zone increases when K increases, and decreases with increasing L and W. White and Falkland (2010) used this relationship to estimate the thickness of usable fresh water (H_{WU}), as: $H_{WU} = H_U - \delta/2$. Hence, for there to be usable fresh water, $\delta < 2H_U$, or:

$$\frac{W}{K} > \frac{1}{2}\left(\frac{\alpha D}{2LK}\right)^{1/2} \quad (13)$$

4.2. Numerical models of FGLs

The limitations of analytical solution approaches are overcome through the application of numerical solutions of the density-dependent groundwater flow and solute transport equations that govern FGL dynamics on atoll islands. Numerical models have been applied to investigate a wide range of

field cases of FGLs, and to analyse the processes that impact FGLs in a more general sense. Table 1 lists a selection of numerical modelling case studies of atoll island aquifers. Table 2 summarises the parameter values used within the numerical models listed in Table 1. The list of cases in Table 1 highlights the wide range of objectives for which numerical modelling has been applied, although sustainable yield analysis has been the primary goal. The majority of models have been developed in two-dimensional (2D) cross section because most atoll islands are elongated and this simplification is often reasonable, although Ghassemi et al. (1996) found that a three-dimensional (3D) model was necessary to reproduce important processes influencing Nauru's FGL. SUTRA and SEAWAT (in 2D and 3D, respectively) have been the preferred models for simulating atoll island FGLs.

Table 1. *Examples of atoll island numerical modelling studies.*

Field site	Authors	Code used (Dimension)	Description
Enjebi Island, Enewetak Atoll, Marshall Islands	Oberdorfer et al. (1990)	SUTRA (2D)	Considering tidal boundary conditions, a two-aquifer model of the island was calibrated to field observations, providing insights into tidal and heterogeneity effects, mixing zone processes and optimal values of dispersivity (i.e. 0.02 m).
Laura Island, Majuro Atoll, Marshall Islands	Griggs and Peterson (1993)	SUTRA (2D)	Two-layer model of the island was used to conduct parametric sensitivity analyses, and to evaluate pumping strategies for optimal freshwater extraction.
Nauru Island, Nauru	Ghassemi et al. (1996)	SUTRA (2D) and HST3D (3D)	The study compared the performance of SUTRA and HST3D for simulating the FGL of Nauru Island, in 2D and 3D, respectively. A total rate of skimming well pumping of 400 m^3/d was recommended.
Bonriki lens, Tarawa Atoll, Kiribati	Alam and Falkland (1997)	SUTRA (2D)	Various climate change scenarios were evaluated for the Bonriki FGL. The impact of rainfall reduction was found to be quite severe.
Home Island, Cocos (Keeling) Islands	Ghassemi et al. (1999)	SALTFLOW (3D)	A two-layer model was developed to assess allowable pumping from the Home Island FGL. Modelling results indicated an upper limit of 200 m^3/d.
Bonriki and Buota lenses, Tarawa Atoll, Kiribati	Alam et al. (2002)	SUTRA (2D)	Two layer models of the lenses, both with and without tides, were developed to assess allowable pumping rates. Modelling results indicate sustainable limits of 345 m^3/d and 1660 m^3/d for Buota and Bonriki lenses, respectively.
Mba Island, Noumea lagoon, New Caledonia	Comte et al. (2010)	SEAWAT (3D) and SUTRA (2D)	Two-layer models in 2D (SUTRA) and 3D (SEAWAT) are compared to resistivity profiles to estimate the water balance (recharge minus evapotranspiration) of Mba Island. Recharge was found to exceed evapotranspiration on higher topographical areas, where the reverse was true for lower areas.
Maldives (201 islands)	Bailey et al. (2014)	SUTRA (2D)	This study uses 6 island widths, 3 latitudinal belts, and two-layer aquifers to represent the known range of parameters for 201 Maldivean island settings, albeit pumping was neglected. FGL thicknesses were compared to observed values for 22 islands. Major variations in FGL thickness were obtained during 1998–2011.
Laura Island, Majuro Atoll, Marshall Islands	Guha (2010)	SEAWAT (3D)	A three-layer model of Laura Island was developed. Tides were represented simply by an increased dispersivity. The model was used for sea-level rise scenarios.

Table 2. *Parameter values of atoll island numerical modelling studies.*

Parameter	Oberdorfer et al. (1990)	Griggs and Peterson (1993)	Ghassemi et al. (1996)	Alam and Falkland (1997)	Ghassemi et al. (1999)	Alam et al. (2002)	Comte et al. (2010)	Bailey et al. (2014)	Guha (2010)
Porosity (-)	0.3	0.2–0.3	0.3	0.3	0.3	0.2	0.2–0.3	0.2–0.3	0.2
Holocene sediments thickness (m)	12	-	-	12	12	15	-	13–18	15
Holocene sediments; horizontal hydraulic conductivity (md^{-1})	10	17	900	5	10	6–12	10	75	70
Holocene sediments; vertical hydraulic conductivity (md^{-1})	-	-	18	1	2	1.2–2.4	7	15	7
Pleistocene sediments; horizontal hydraulic conductivity (md^{-1})	1000	170	900	500	500	500	900	5000	700
Pleistocene sediments; vertical hydraulic conductivity (md^{-1})	-	-	18	100	100	100	180	1000	70
Longitudinal dispersivity (m)	0.02	15	65	10	5	8	0.7	6	3
Transverse dispersivity (m)	0	0.01	0.15	1	1	1	0.02	0.05	0.2
Average annual recharge (mm)	500	1780	540	855	855	926–980	50–300	655–935	-

Aside from modelling case studies (e.g. Table 1) a number of numerical modelling investigations have been completed to investigate specific FGL processes of atoll islands. For example, Bailey et al. (2009) adopted Ayers and Vacher's (1986) general conceptual model for atoll island aquifers in a 2D SUTRA model to assess sensitivities of FGL characteristics to various aquifer parameters. Seasonal rainfall patterns and tidal boundary conditions were considered. The authors found, among other interpretations, that the *K* of the Holocene sediments was 50 m/d and 400 m/d in leeward and windward islands, respectively, and hence the prevailing wind direction has a strong influence on FGL. Following a six-month drought, they concluded that the recovery period for FGLs was on the order of 1.5 years. Underwood et al. (1992) also completed a generalised atoll island numerical investigation. Among other findings mentioned above in relation to their study, they showed that the vertical flow within atoll islands, generated by tides and the characteristic layered geology, is an important function in the widening of the transition zone. Hence, where tides are neglected, a larger transverse dispersivity is needed to reproduce observed transition zone thicknesses (Underwood et al. 1992).

5. References

Abarca E., Carrera J., Sanchez-Vila X. and Dentz, M. 2007. Anisotropic dispersive Henry problem. Advances in Water Resources 30:913–926.

Alam K. and Falkland A.C. 1997. Vulnerability to climate change of the Bonriki freshwater lens, Tarawa. Ministry of Environment and Social Development, Republic of Kiribati. ECOWISE Environmental Pty Ltd, and ACTEW Corporation. 55 p.

Alam K., Falkland A. and Mueller N. 2002. Sustainable yield of Bonriki and Buota freshwater lenses, Tarawa. In: Project S. (ed). Hydrogeology Component. ECOWISE Environmental Pty Ltd.

Anderson Jr, W.P. and Lauer R.M. 2008. The role of overwash in the evolution of mixing zone morphology within barrier islands. Hydrogeology Journal 16:1483–1495.

Ataie-Ashtiani B., Rajabi M.M. and Ketabchi H. 2013. Inverse modelling for freshwater lens in small islands: Kish Island, Persian Gulf. Hydrological Processes 27:2759–2773.

Ayers J.F. and Vacher H.L. 1986. Hydrogeology of an Atoll Island: A conceptual model from detailed study of a Micronesian example. Ground Water 24:185–198.

Bailey R.T. and Jenson J.W. 2014. Effects of marine overwash for atoll aquifers: Environmental and human factors. Ground Water 52(5):694–704, doi:10.1111/gwat.12117.

Bailey R.T., Jenson J.W., Rubinstein D. and Olsen A.E. 2008. Groundwater resources of atoll islands: Observations, modelling and management. Water and Environmental Research Institute of the Western Pacific, University of Guam. 84 p.

Bailey R.T., Jenson J.W. and Olsen A.E. 2009. Numerical modeling of atoll island hydrogeology. Ground Water 47: 184–196.

Bailey R.T., Jenson J.W. and Olsen A.E. 2010. Estimating the ground water resources of atoll islands. Water 2:1–27.

Bailey R.T., Khalil A. and Chatikavanij V. 2014. Estimating transient freshwater lens dynamics for atoll islands of the Maldives. Journal of Hydrology 515:247–256.

Bricker S.H. 2009. Impacts of climate change on small island hydrogeology — A literature review. Groundwater Sciences Programme, Open Report OR/09/025. Nottingham: British Geological Survey. 28 p.

Buddemeier R.W. and Oberdorfer J.A. 1986. Internal hydrology and geochemestry of coral reefs and atoll islands: Key to diagenetic variations. In: Schroeder J.H. and Purser B.H. (eds). Reef Diagenesis. Berlin: Springer-Verlag.

Buddemeier R.W. and Oberdorfer J.A. 1997. Hydrogeology of Enewetak Atoll. In: Vacher, H.L. and Quinn, T.M. (eds). Geology and hydrogeology of carbonate islands. Developments in Sedimentology 54, Chapter 22, p. 667–692, Amsterdam: Elsevier.

Chui T.F.M. and Terry J.P. 2012. Modeling fresh water lens damage and recovery on atolls after storm-wave washover. Ground Water 50:412–420.

Chui T.F.M. and Terry J.P. 2013. Influence of sea-level rise on freshwater lenses of different atoll island sizes and lens resilience to storm-induced salinization. Journal of Hydrology 502: 18–26.

Comte J.-C., Banton O., Join J.-L. and Cabioch G. 2010. Evaluation of effective groundwater recharge of freshwater lens in small islands by the combined modeling of geoelectrical data and water heads. Water Resources Research 46, W06601.

Cooper H.H.J. 1964. A hypothesis concerning the dynamic balance of fresh water and salt water in a coastal aquifer. Journal of Geophysical Reseach 64:461–467.

Custodio E. and Bruggeman G.A. 1987. Studies and reports in hydrology: Groundwater problems in coastal areas. Paris, France: United Nations Educational, Scientific and Cultural Organization. 610 p.

Falkland A. 1991. Hydrology and water resources of small islands: A practical guide. A contribution to the International Hydrological Programme. Paris, France: United Nations Educational, Scientific and Cultural Organization. 453 p.

Falkland A. 1992a. Small tropical islands: Water resources of paradises lost. Water-related issues and problems of the humid tropics and other warm humid regions. United Nations Educational, Scientific and Cultural Organization. 51 p.

Falkland A.C. 1992b. Review of Tarawa freshwater lenses, Republic of Kiribati. Report HWR92/681. Hydrology and Water Resources Branch, ACT Electricity and Water. Prepared for the Australian International Development Assistance Bureau.

Falkland A.C. and Woodroffe C.D. 1997. Geology and hydrogeology of Tarawa and Christmas islands, Kiribati. In: Vacher H.L. and Quinn T.M. (eds). Geology and hydrogeology of carbonate islands. Developments in Sedimentology 54, Chapter 19, p. 577–610, Amsterdam: Elsevier.

Ferris J.G. 1951. Cyclic fluctuations of water levels as a basis for determining aquifer transmissibility. Washington: US Geological Survey, Water Resources Division.

Fetter C.W. 1972. Position of the saline water interface beneath oceanic islands. Water Resources Research 8: 1307–1315.

Gelhar L.W., Welty C. and Rehfeldt K.R. 1992. A critical review of data on field-scale dispersion in aquifers. Water Resources Research 28:1955–1974.

Ghassemi F., Jakeman A.J., Jacobson G. and Howard K.W.F. 1996. Simulation of seawater intrusion with 2D and 3D models: Nauru Island case study. Hydrogeology Journal 4: 4–22.

Ghassemi F., Molson J.W., Falkland A. and Alam K. 1999. Three-dimensional simulation of the Home Island freshwater lens: preliminary results. Environmental Modelling and Software 14:181–190.

Gingerich S.B. and Voss C.I. 2014. Sea-level rise and seawater inundation of an atoll island, Roi-Namur, Kwajalein Atoll, Republic of the Marshall Islands. In: Wiederhold H., Michaelsen J., Hinsby K.

and Nommensen B. (eds). SWIM 2014, 23rd Salt Water Intrusion Meeting, 16–20 June 2014, pp. 129–131, Husum, Germany, ISBN: 978-3-00-046061-6.

Glover R.E. 1959. The pattern of fresh-water flow in a coastal aquifer. Journal of Geophysical Research 64:457–459.

Griggs J.E. and Peterson F.L. 1993. Ground-water flow dynamics and development strategies at the atoll scale. Ground Water 31:209–220.

Guha S. 2010. Variable-density flow models of saltwater intrusion in coastal landforms in response to climate change induced sea-level rise and a chapter on time-frequency analysis of ground penetrating radar signals. Ph.D. dissertation, University of Florida. 183 p. http://scholarcommons.usf.edu/etd/3490

Hoeke R.K., McInnes K.L., Kruger J.C., McNaught R.J., Hunter J.R. and Smithers S.G. 2013. Widespread inundation of Pacific islands triggered by distant-source wind-waves. Global and Planetary Change 108:128–138.

Holding S.T. and Allen D.M. 2014. Responses to climate change and development stressors on small oceanic islands. In: Wiederhold H., Michaelsen J., Hinsby K. and Nommensen B. (eds). SWIM 2014, 23rd Salt Water Intrusion Meeting, 16–20 June 2014, pp. 129–131, Husum, Germany, ISBN: 978-3-00-046061-6.

Horn D.P. 2006. Measurements and modelling of beach groundwater flow in the swash-zone: a review. Continental Shelf Research 26:622–652.

Hunt Jr C.D. 1997. Hydrogeology of Diego Garcia. p. 909–932. In: Vacher H.L. and Quinn T.M. (eds). Geology and hydrogeology of carbonate islands. Developments in Sedimentology 54, Chapter 32, , Amsterdam: Elsevier.

Hunt Jr C.D. and Peterson F.L. 1980. Groundwater resources of Kwajalein Island, Marshall Islands. Water Resources Research Center, University of Hawaii, Technical Report No. 126, Manoa.101 p.

http://scholarspace.manoa.hawaii.edu/bitstream/handle/10125/2534/wrrctr126.pdf?sequence=1

Illangasekare T., Obeysekera J., Hyndman D.W., Perera L., Vithanage M. and Gunatilaka A. 2009. Impacts of the 2004 tsunami and subsequent water restorations actions in Sri Lanka. In: Illangasekare T.H., Mahutova K. and Barich III J.J. (eds). Decision support for natural disasters and international threats to water supply. NATO Science for Peace and Security Series. Dordrecht: Springer. 251 p.

Illangasekare T., Tyler S.W., Clement T.P., Villholth K.G., Perera A.P.G.R.L., Obeysekera J., Gunatilaka A., Panabokke C.R., Hyndman D.W., Cunningham K.J., Kaluarachchi J.J., Yeh W. W.-G., van Genuchten M.T. and Jensen K. 2006. Impacts of the 2004 tsunami on groundwater resources in Sri Lanka. Water Resources Research 42, W05201.

Jacobson G., Hill P.H. and Ghassemi F. 1997. Geology and hydrogeology of Nauru Island. p. 707–742. In: Vacher H.L. and Quinn T.M. (eds). Geology and hydrogeology of carbonate islands. Developments in Sedimentology 54, Chapter 24, Amsterdam: Elsevier.

Kerrou J. and Renard P. 2010. A numerical analysis of dimensionality and heterogeneity effects on advective dispersive seawater intrusion processes. Hydrogeology Journal 18:55–72.

Ketabchi H., Mahmoodzadeh D., Ataie-Ashtiani B., Werner A.D. and Simmons C.T. 2014. Sea-level rise impact on fresh groundwater lenses in two-layer small islands. Hydrological Processes, doi:10.1002/hyp.10059.

KNSO and SPC 2012. Kiribati 2010 census. Volume 2, Analytical report. Kiribati National Statistics Office and the Secretariat of the Pacific Community Statistics for Development Program.

Lu C., Chen Y., Zhang C. and Luo J. 2013. Steady-state freshwater–seawater mixing zone in stratified coastal aquifers. Journal of Hydrology 505:24–34.

Lu C., Kitanidis P.K. and Luo J. 2009. Effects of kinetic mass transfer and transient flow conditions on widening mixing zones in coastal aquifers. Water Resources Research 45, W12402.

Marshall J.F. and Jacobson G. 1985. Holocene growth of a mid-Pacific atoll: Tarawa, Kiribati. Coral Reefs 4:11–17.

Moore W.S. 1999. The subterranean estuary: a reaction zone of ground water and sea water. Marine Chemistry 65:111–125.

Morgan L.K. and Werner A.D. 2014. Seawater intrusion vulnerability indicators for freshwater lenses in strip islands. Journal of Hydrology 508:322–327.

Mulligan A.E., Langevin C. and Post V.E. 2011. Tidal boundary conditions in SEAWAT. Ground Water 49:866–879.

Oberdorfer J.A., Hogan P.J. and Buddemeier R.W. 1990. Atoll island hydrogeology: Flow and freshwater occurrence in a tidally dominated system. Journal of Hydrology 120:327–340.

Peterson F.L. 1997. Hydrogeology of the Marshall Islands. p. 611–636. In: Vacher H.L. and Quinn T.M. (eds). Geology and hydrogeology of carbonate islands. Developments in Sedimentology 54, Chapter 20. Amsterdam: Elsevier.

Post V.E.A. 2011. A new package for simulating periodic boundary conditions in MODFLOW and SEAWAT. Computers and Geosciences 37:1843–1849.

Ritzi R.W. Jr, Bukowski J.M., Carney C.K. and Boardman M.R. 2001. Explaining the thinness of the fresh water lens in the Pleistocene carbonate aquifer on Andros Island, Bahamas. Ground Water 39:713–720.

Robinson C., Gibbes B. and Li L. 2006. Driving mechanisms for groundwater flow and salt transport in a subterranean estuary. Geophysical Research Letters 33, L03402.

Robinson C., Li L. and Barry D.A. 2007. Effect of tidal forcing on a subterranean estuary. Advances in Water Resources 30:851–865.

Schneider J.C. and Kruse S.E. 2003. A comparison of controls on freshwater lens morphology of small carbonate and siliciclastic islands: examples from barrier islands in Florida, USA. Journal of Hydrology 284:253–269.

Stoddart D.R. and Cann J.R. 1965. Nature and origin of beach rock. Journal of Sedimentary Petrology 35:243–273.

Strack O.D.L. 1989. Groundwater mechanics. Englewood Cliffs: Prentice Hall. 732 p. (out of print, currently published by Strack Consulting, Inc.).

Terry J.P. and Chui T.F.M. 2012. Evaluating the fate of freshwater lenses on atoll islands after eustatic sea-level rise and cyclone-driven inundation: A modelling approach. Global and Planetary Change 88–89, 76–84.

Terry J.P. and Falkland A.C. 2010. Responses of atoll freshwater lenses to storm-surge overwash in the Northern Cook Islands. Hydrogeology Journal 18:749–759.

Turner I.L. 1995. Modelling the time-varying extent of groundwater seepage on tidal beaches. Earth Surface Processes and Landforms 20:833–843.

Underwood M.R., Peterson F.L. and Voss C.I. 1992. Groundwater lens dynamics of atoll islands. Water Resources Research 28:2889–2902.

Vacher H.L. 1988. Dupuit-Ghyben-Herzberg analysis of strip-island lenses. Geological Society of American Bulletin 100:580–591.

Vacher H.L. 1997. Varieties of carbonate islands and a historical perspective. p. 1–34. In: Vacher H.L. and Quinn T.M. (eds). Geology and hydrogeology of carbonate islands. Developments in Sedimentology 54, Chapter 1. Amsterdam: Elsevier.

Vacher H.L. and Rowe M.P. 1997. Geology and hydrogeology of Bermuda. p. 35–90. In*:* Vacher H.L. and Quinn T.M. (eds). Geology and hydrogeology of carbonate islands. Developments in Sedimentology 54, Chapter 2. Amsterdam: Elsevier.

Van der Veer P. 1977. Analytical solution for steady interface flow in a coastal aquifer involving a phreatic surface with precipitation. Journal of Hydrology 34:1–11.

Violette S., Boulicot G. and Gorelick S.M. 2009. Tsunami-induced groundwater salinization in southeastern India. C. R. Geoscience 341:339–346.

Volker R.E., Marino M.A. and Rolston D. 1985. Transition zone width in ground water on ocean atolls. Journal of Hydraulic Engineering 111:659–676.

Weber J.N. and Woodhead M.J. 1972. Carbonate lagoon and beach sediments of Tarawa Atoll, Gilbert Islands. Atoll Research Bulletin 157. Washington: The Smithsonian Institution.

Werner A.D., Bakker M., Post V.E.A., Vandenbohede A., Lu C., Ataie-Ashtiani B., Simmons C.T. and Barry D.A. 2013a. Seawater intrusion processes, investigation and management: Recent advances and future challenges. Advances in Water Resources 51:3–26.

Werner A.D., Jacobsen P.E. and Morgan L.K. 2013b. Understanding seawater intrusion. [Poster]. Earth Sciences collection, http://hdl.handle.net/2328/26647. Flinders Academic Commons, Adelaide, South Australia.

Werner A.D. and Lockington D.A. 2006. Tidal impacts on riparian salinities near estuaries. Journal of Hydrology 328:511–522.

Werner A.D. and Simmons C.T. 2009. Impact of sea-level rise on seawater intrusion in coastal aquifers. Ground Water 47:197–204.

Werner A.D., Ward J.D., Morgan L.K., Simmons C.T., Robinson N.I. and Teubner M.D. 2012. Vulnerability indicators of sea water intrusion. Ground Water 50:48–58.

White I. and Falkland T. 2010. Management of freshwater lenses on small Pacific islands. Hydrogeology Journal 18:227–246.

White I., Falkland T., Perez P., Dray A., Metutera T., Metai E. and Overmars M. 2007. Challenges in freshwater management in low coral atolls. Journal of Cleaner Production 15:1522–1528.

Woodroffe C.D. 2008. Reef-island topography and the vulnerability of atolls to sea-level rise. *Global and Planetary Change*, 62, 77-96.

Woodroffe C.D. and Falkland A.C. 1997. Geology and hydrogeology of the Cocos (Keeling) Islands. p. 885–908. In: Vacher H.L. and Quinn T.M. (eds). Geology and hydrogeology of carbonate islands. Developments in Sedimentology 54, Chapter 31. Amsterdam: Elsevier.

CONTACT DETAILS
Secretariat of the Pacific Community

SPC Headquarters
BP D5,
98848 Noumea Cedex,
New Caledonia
Telephone: +687 26 20 00
Fax: +687 26 38 18

SPC Suva Regional Office
Private Mail Bag,
Suva,
Fiji,
Telephone: +679 337 0733
Fax: +679 337 0021

SPC Pohnpei Regional Office
PO Box Q,
Kolonia, Pohnpei, 96941 FM,
Federated States of Micronesia
Telephone: +691 3207 523
Fax: +691 3202 725

SPC Solomon Islands
Country Office
PO Box 1468
Honiara, Solomon Islands
Telephone: + 677 25543 /
+677 25574
Fax: +677 25547

Email: spc@spc.int
Website: www.spc.int